Fine-scale fluctuations of PM_1, $PM_{2.5}$, PM_{10} and SO_2 concentrations caused by a prolonged volcanic eruption (Fagradalsfjall 2021, Iceland)

Rachel C. W. Whitty[1], Evgenia Ilyinskaya[1], Melissa A. Pfeffer[2], Ragnar H. Thrastarson[2], Þorsteinn Johannsson[3], Sara Barsotti[2], Tjarda J. Roberts[4, 5], Guðni M. Gilbert[2, 9], Tryggvi Hjörvar[2], Anja Schmidt[6, 7, 8], Daniela Fecht[10], Grétar G. Sæmundsson[11]

[1]COMET, Institute of Geophysics and Tectonics, School of Earth and Environment, University of Leeds, Leeds, LS2 9JT, United Kingdom

[2]Icelandic Meteorological Office, 150 Reykjavík, Iceland

[3]The Environment Agency of Iceland, 108 Reykjavík, Iceland

[4]CNRS UMR7328, Laboratoire de Physique et de Chimie de l'Environnement et de l'Espace, Universite d'Orleans, Orleans, 45071, France

[5]LMD/IPSL, ENS, Université PSL, École Polytechnique, Institute Polytechnique de Paris, Sorbonne Université, CNRS, F-75005 Paris, France

[6]Yusuf Hamed Department of Chemistry, University of Cambridge, Cambridge, CB2 1EW, United Kingdom

[7]Institute of Atmospheric Physics (IPA), German Aerospace Centre (DLR), 82234 Oberpfaffenhofen, Germany

[8]Meteorological Institute, Ludwig Maximilian University of Munich, 80333 Munich, Germany

[9]Nox Medical, 150 Reykjavík, Iceland

[10]MRC Centre for Environment and Health, School of Public Health, Imperial College London, London, W12 0BZ, United Kingdom

[11]Department of Research and Analysis, Icelandic Tourist Board, 101 Reykjavík, Iceland

Correspondence to: Evgenia Ilyinskaya (e.ilyinskaya@leedss.ac.uk)

Abstract

The 2021 Fagradalsfjall eruption marked the first in a series of ongoing eruptions in a densely populated region of Iceland (> 260,000 residents within 50 km distance). This eruption was monitored by an exceptionally dense regulatory air quality network, providing a unique opportunity to examine fine-scale dispersion patterns of volcanic air pollutants (SO_2, PM_1, $PM_{2.5}$, PM_{10}) in populated areas.

Despite its relatively small size, the eruption led to statistically-significant increases in both average and peak concentrations of PM and SO_2 at distances of at least 300 km. Peak daily-mean concentrations of PM_1 rose from 5–6 μg/m³ to 18–20 μg/m³,

and the proportion of PM_1 within PM_{10} increased by ~50%. In areas with low background pollution, PM_{10} and $PM_{2.5}$ levels increased by ~50% but in places with high background sources, the eruption's impact was not detectable. These findings suggest that ash-poor eruptions are a major source of PM_1 in Iceland and potentially in other regions exposed to volcanic emissions.

Air quality thresholds for all measured pollutants were exceeded more frequently during the eruption than under background conditions. This suggests a possible increase in adverse health effects. Moreover, pollutant concentrations exhibited strong fine-scale temporal (≤1 hour) and spatial (<1 km) variability. This suggests disparities in population exposures to volcanic air pollution, even from relatively distal sources (20–55 km distance), and underscores the importance of a dense monitoring network and effective public communication.

1 Introduction

Airborne volcanic emissions—commonly referred to as 'volcanic air pollution'—pose both acute and chronic health hazards that can affect populations across large geographic areas (Stewart et al., 2021, and references within). Globally, over one billion people are estimated to live within 100 km of an active volcano (Freire et al., 2019), a distance within which they might be exposed to volcanic air pollution (Stewart et al., 2021). The number of potentially exposed people is growing, for example, due to building expansion into previously uninhabited areas near volcanoes. In this study, we examine the impacts of volcanic emissions on air quality in populated areas using high-resolution, high-quality observational data. We focus on the 2021 Fagradalsfjall fissure eruption on the Reykjanes Peninsula as a case study. Fissure eruptions are one of the most common types of volcanic activity that affects air quality. Recent examples of fissure eruptions at the urban interface include the Kīlauea volcano in Hawai'i (with tens of episodes since 1983), Cumbre Vieja on La Palma in 2021, and the Reykjanes Peninsula in Iceland (11 eruptions since 2021). Fissure eruptions have low explosivity and produce negligible ash but release prodigious amounts of gases and aerosol particulate matter close to ground level. Even small fissure eruptions can cause severe air pollution episodes (Whitty et al., 2020).

Fine-scale spatial variability in air pollutant concentrations—characterized by steep gradients over distances of just a few kilometres or less—is currently one of the most active areas of research within the broader field of air pollution (Apte and Manchanda, 2024). In urban areas, these fine-scale variations contribute to disparities in air quality, population exposure, and associated physical, mental, and social well-being (Apte and Manchanda, 2024, and references within). The 2021 Fagradalsfjall eruption provided a novel opportunity to investigate the fine-scale variability of volcanic air pollution in urban settings, as it was monitored by an exceptionally dense regulatory air quality network. Here, we use the term 'regulatory' to describe an air quality monitoring network operated by a national agency, employing certified commercial instrumentation with regulated setup and calibration protocols. These networks provide high-accuracy, high-precision measurements with high temporal resolution, but typically with low spatial resolution due to the high costs of installation (typically > € 100,000) and maintenance

(typically > € 100,000 per annum). For example, Germany has approximately one regulatory station per ~250,000 people, with a similar density in the United States (Apte and Manchanda, 2024). In many volcanic regions, regulatory air quality monitoring is either absent or very sparse (Felton et al., 2019). Prior to our study, the best-observed case studies of volcanic air pollution came from Kīlauea volcano in Hawaii (in particular, its large fissure eruption in 2018), and the large Holuhraun fissure eruption 2014-2015 in Iceland (Crawford et al., 2021; Gíslason et al., 2015; Ilyinskaya et al., 2017; Schmidt et al., 2015; Whitty et al., 2020). These events were monitored by relatively few and distant regulatory stations—approximately 90 km from the eruption site at Holuhraun and about 40 km at Kīlauea. In contrast, the 2021 Fagradalsfjall eruption occurred in Iceland's most densely populated region and in response, national authorities made a strategic decision early on to expand the regulatory network, ensuring that nearly every community was covered by at least one station. During the eruption, 27 regulatory stations were operational across Iceland, with 14 located within 40 km of the eruption site. Some stations were positioned less than 1 km apart, enabling unprecedented spatial resolution in observing volcanic air pollution.

Regulatory air quality networks can be supplemented by so-called lower-cost sensors (LCS), which are typically small in size (a few centimetres) and cost approximately € 200. An active body of research on the expanding use of LCS highlights their potential to enhance the relatively sparse regulatory networks (reviewed in Apte and Manchanda, 2024; and Sokhi et al., 2022). For example, during a two-week campaign in 2018, the regulatory air quality network on Hawai'i Island was augmented with 16 LCS. This denser network significantly changed the estimates of population exposure to volcanic air pollution (Crawford et al., 2021). Despite their advantages in affordability and portability, LCS have notable limitations, including relatively poor accuracy and precision compared to regulatory-grade instruments, and a lack of standardised protocols for installation and maintenance. In our study, LCS were deployed to establish a rapid-response monitoring network directly at the eruption site, aimed at mitigating exposure hazards for the approximately 300,000 visitors who came to view the eruption. We present and discuss the use of LCS in a crisis mitigation context, which has broader relevance for other high-concentration, rapid-onset air pollution events, such as wildfires.

1.1 Volcanic air pollutants and associated health impacts

Much of the existing knowledge on the health impacts of volcanic air pollution comes from epidemiological and public health investigations of the eruptions at Holuhraun in Iceland and Kīlauea in Hawaii. The Holuhraun eruption was associated with increased healthcare utilisation for respiratory conditions in the country's capital area, located approximately 250 km from the eruption site (Carlsen et al., 2021a, b). These findings are consistent with observations from Kīlauea on Hawaii, which have been based on more qualitative health assessments and questionnaire-based surveys (Horwell et al., 2023; Longo, 2009; Longo et al., 2008; Tam et al., 2016). Volcanic emissions contain a wide array of chemical species, many of which are hazardous to human health (reviewed in Stewart et al., 2021). In this study, we focus on sulfur dioxide gas (SO_2) and three particulate matter (PM) size fractions— PM_1, $PM_{2.5}$, PM_{10}—which refer to particles with aerodynamic diameters less than 1 μm, 2.5 μm, and 10 μm, respectively. These pollutants are typically elevated both near the eruption source and at considerable distances downwind

(Stewart et al., 2021). Throughout this work, we use the term 'volcanic emissions' to refer collectively to SO_2 and PM, unless otherwise specified.

Sulfur dioxide is abundant in volcanic emissions and a key air pollutant in volcanic areas (Crawford et al., 2021; Gíslason et al., 2015; Ilyinskaya et al., 2017; Schmidt et al., 2015; Whitty et al., 2020). Laboratory studies have shown that individuals with asthma are particularly sensitive to even relatively low concentrations of SO_2 (below 500 μg/m³), and air quality thresholds are typically established to protect this vulnerable group (US EPA National Center for Environmental Assessment, 2008). Epidemiological studies in volcanic regions further indicate that children (defined as ≤4 years old) and the elderly (≥64 years old) are more susceptible to adverse health effects from above-threshold SO_2 exposure compared to the general adult population (Carlsen et al., 2021b). In recent decades, the number of regulatory air quality stations monitoring SO_2 has declined across much of the Global North, largely due to reductions in anthropogenic emissions, particularly from coal combustion. To our knowledge, Iceland currently maintains the highest number and spatial density of regulatory SO_2 monitoring stations worldwide. This study therefore provides an unprecedented spatial resolution of SO_2 exposure in a densely populated, modern society affected by this pollutant.

Volcanic emissions are extremely rich in PM, comprising both primary particles emitted directly from the source and secondary particles formed through post-emission processes, such as sulfur gas-to-particle conversion. All three PM size fractions reported in this study— PM_1, $PM_{2.5}$, PM_{10}—are known to be significantly elevated near volcanic sources. In fissure eruptions, PM_1 is typically the dominant size fraction (Ilyinskaya et al., 2012, 2017; Mather et al., 2003). Exposure to PM air pollution, from natural and anthropogenic sources, has been linked to a wide range of adverse health outcomes, including cardiovascular and respiratory diseases, and lung cancer (Brauer et al., 2024, and references within). Health impacts have been observed even at low concentrations, with children and the elderly particularly vulnerable. The size of PM plays a critical role in determining health impacts. $PM_{2.5}$ has long been associated with worse health outcomes compared to PM_{10} (Janssen et al., 2013; McDonnell et al., 2000), and the importance of PM_1 is now a key focus in air pollution and health research. Multiple epidemiological studies from China have found PM_1 exposure to be more strongly correlated with negative health outcomes than $PM_{2.5}$ (Gan et al., 2025; Guo et al., 2022; Yang et al., 2018; Zhang et al., 2020). In Europe, epidemiological research on PM_1 health impacts is still in its early stages (Tomášková et al., 2024), largely due to a lack of high-quality observational data on PM_1 concentrations and exposure. This study contributes the first regulatory-grade time series and exposure dataset of PM_1 from a volcanic source, as well as the first measurements of PM_1 in Iceland.

In volcanic emissions, concentrations of both SO_2 and PM in various size fractions are consistently elevated, but their relative proportions vary depending on several factors, including distance from the source, plume age, and the rate of gas-to-particle conversion. Existing evidence suggests that this variability in plume composition may influence the associated health outcomes in distinct ways. An epidemiological study in Iceland comparing SO_2-dominated plumes with PM-dominated plumes found that the latter was associated with a greater increase in the dispensation of asthma medication and reported cases of respiratory infections (Carlsen et al., 2021a). In contrast, statistically significant increases in healthcare utilization for chronic obstructive pulmonary disease (COPD) were observed only in association with exposure to SO_2-dominated plumes (Carlsen et al., 2021a).

Our study contributes a dataset on different types of volcanic air pollutants with a higher spatial resolution than has been previously been possible. This offers a foundation for future epidemiological research into the health impacts of recent and ongoing eruptions in Iceland.

1.2 Fagradalsfjall 2021 eruption

The 2021 Fagradalsfjall eruption (19 March - 19 September 2021) was the first volcanic event on the Reykjanes peninsula in nearly 800 years. This region is the most densely populated area of Iceland, with over 260,000 people—around 70% of the national population—residing within 50 km of the eruption site. The eruption site was 9 km from the town of Grindavík and approximately 25 km from the capital area of Reykjavík (Fig. 1). Although the eruption took place in an uninhabited area, it attracted an estimated 300,000 visitors who observed the event at close range.

The eruption was a basaltic fissure eruption with an effusive and mildly explosive style, dominated by lava fountaining and lava flows (Barsotti et al., 2023). While relatively small in size—emitting a total of ~0.3–0.9 Mt of SO_2 and covering an area of 4.82 km² with lava (Barsotti et al., 2023; Pfeffer et al., 2024)—its proximity to urban areas and the high number of visitors likely resulted in greater population exposure to volcanic air pollution than any previous eruption in Iceland.

This eruption is considered to mark the onset of a new period of frequent eruptions on the Reykjanes peninsula. Such periods, locally referred to as the 'Reykjanes Fires', have occurred roughly every 1000 years, each lasting for decades to centuries. The last period of Reykjanes Fires ended with an eruption in 1240 CE (Sigurgeirsson and Einarsson, 2019). Since the 2021 eruption, ten further eruptions have occurred on the Reykjanes peninsula: two within the Fagradalsfjall volcanic system (August 2022 and July 2023), and eight within the adjacent Reykjanes-Svartsengi system (December 2023 to April 2025). Volcanic unrest continues at the time of writing, and based on the eruption history of the Reykjanes peninsula, further eruptions may occur repeatedly over the coming decades or centuries.

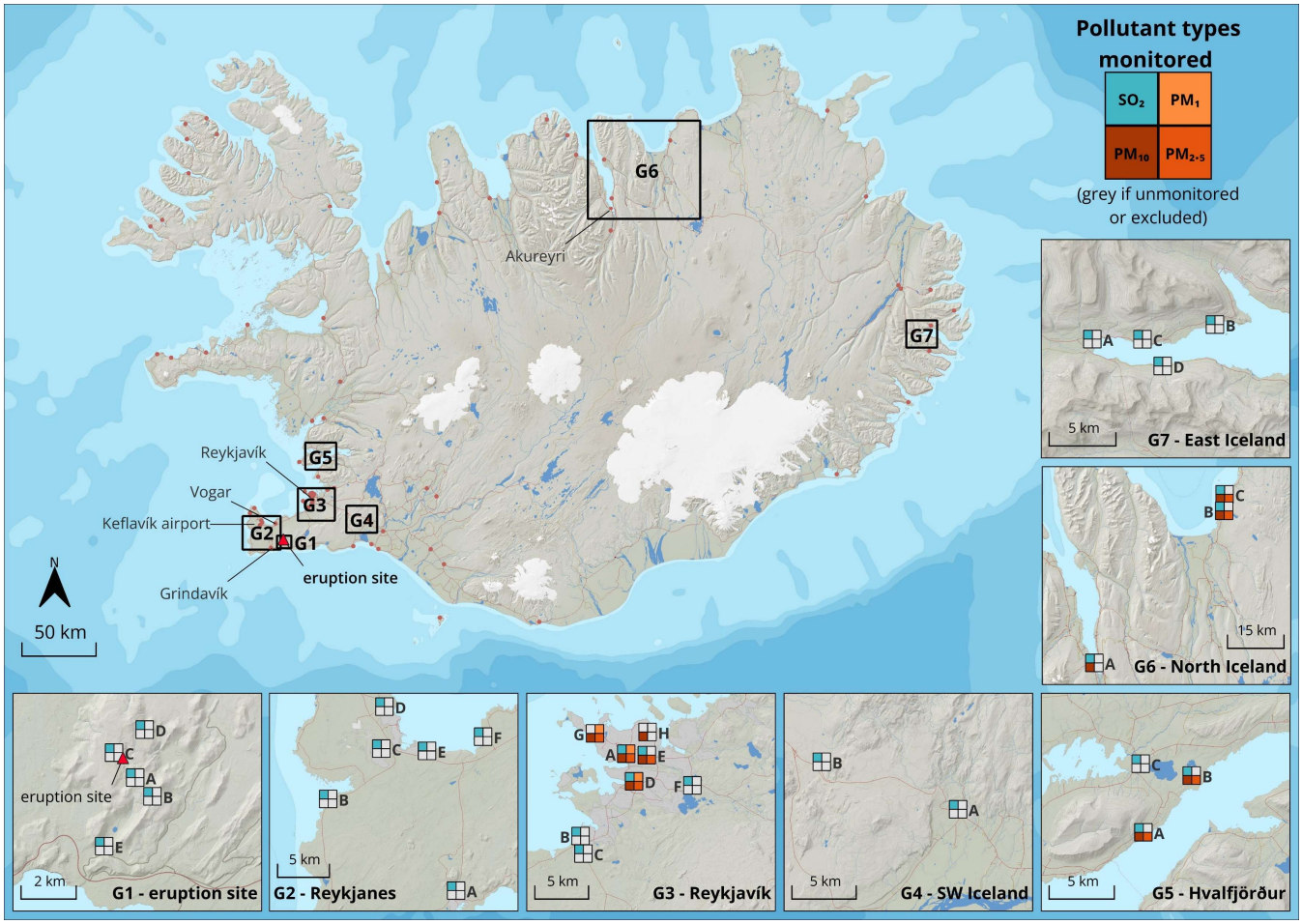

Figure 1: Map of Iceland showing the eruption site and air quality monitoring stations. The stations were organised in seven geographic clusters (each shown on the enlarged insets). G1 - Eruption site (0-4 km from the eruption site). G2 - Reykjanes peninsula (9-20 km). G3 - Reykjavík capital area (25-35 km). G4 - Southwest Iceland (45-55 km). G5 - Hvalfjörður (50-55 km). G6 - North Iceland (A and B ~280 km; C and D ~330 km). G7 - East Iceland (~400 km). The map shows the air pollutant species monitored at each station (SO_2, PM_{10}, $PM_{2.5}$, PM_1). Areas G2-G7 were monitored with regulatory stations, while G1 was monitored using lower-cost eruption response sensors. Source and copyright of basemap and cartographic elements: Icelandic Met Office & Icelandic Institute of Natural History.

2 Methods

Data were collected by two types of instrument networks:

1. A regulatory municipal air quality (AQ) network, managed by the Environmental Agency of Iceland (EAI), which measured SO_2 and particulate matter (PM) in different size fractions.
2. An eruption-response lower-cost sensor (LCS) network measuring SO_2 only, operated by the Icelandic Meteorological Office (IMO).

2.1 Regulatory municipal network

The regulatory network monitors air quality across Iceland in accordance with national legal mandates and complies with Icelandic Directive (ID) regulations. Most of the monitoring stations are located in populated areas and measure a variety of air pollutants. Here, we analysed SO_2 and PM in the PM_1, $PM_{2.5}$, and PM_{10} size fractions, which are the most important volcanic air pollutants with respect to human health in downwind populated areas (Stewart et al., 2021). Detection of SO_2 is based on pulsed fluorescence in the ultraviolet, and detection of PM is based on light scattering photometry and beta attenuation. The detection limits for the majority of the stations in this study were reported to be ~1-3 $\mu g/m^3$ SO_2 and < 5 $\mu g/m^3$ PM_{10}. Station-specific instrument details, detection and resolution limits, and operational durations are in Supplementary Table S1. Figure 1 shows the location of the stations and the air pollutants species measured at each site.

2.2 Eruption site sensors

At the eruption site (0.6-3 km from the active craters), the IMO installed a network of five commercially available SO_2 LCS between April and July 2021 to monitor air quality in the near-field. PM was not monitored with this network due to cost-benefit considerations as PM does not pose as acute a hazard as SO_2 for short-term exposure. The sensor specifications and operational durations are detailed in Table S1. Figure 1 shows the location of the eruption-response SO_2 sensor network. Stations A, B, and E were in close proximity to the public footpaths, while stations C and D were further afield to the north and northwest of the eruption site. The main purpose of the eruption-response network was to alert visitors when SO_2 levels were high rather than to provide accurate SO_2 concentrations. This was because LCS are known to be significantly less accurate than regulatory instruments (Crilley et al., 2018; Whitty et al., 2022, 2020). Whitty et al. (2022) assessed the performance of SO_2 LCS specifically in volcanic environments (same or comparable sensor models to those used here) and found that they were frequently subject to interferences restricting their capability to monitor SO_2 in low concentrations. The sensor accuracy identified in the field study by Whitty et al. (2022) was significantly poorer than the detection limits reported by the manufacturer. The sensors used in this study were not calibrated or co-located with higher-grade instruments during the field deployment as this network was set up *ad hoc* as part of an eruption crisis response by IMO. The crisis was two-fold: the eruption itself, and the unprecedented crowding of people who wanted to view the eruption at very close quarters. The purpose of the sensor network was to alert visitors to high and potentially-hazardous concentrations, and it was not intended to produce a regulatory-grade dataset. Furthermore, the 2021 eruption occurred during national and international COVID-19 lockdowns, which reduced the opportunities for field-based research. The lack of a field-based calibration of the sensors significantly limits the accuracy of the obtained LCS data, especially at lower concentration levels. For this reason we analysed the SO_2 data not quantitatively, but as a binary yes/no indicator for exceeding the hourly-mean ID air quality threshold of 350 $\mu g/m^3$. The threshold is ~2 orders of magnitude higher than the manufacturer-reported detection limits and therefore we consider it reasonable to assume that such concentrations would be detectable by the LCS.

2.3 Data processing

SO_2 measurements were downloaded from 24 regulatory stations and 5 eruption site sensors, and PM_{10}, $PM_{2.5}$ and PM_1 were downloaded from 12, 11 and 3 regulatory stations, respectively. Data from the regulatory stations were quality-checked and, where needed, re-calibrated by the EAI. Where the operational duration was sufficiently long, we obtained SO_2 and PM measurements for both the eruption period and the non-eruptive background period.

We excluded from the analysis any regulatory stations that had data missing for more than 4 months of the eruption period (>70%). Further details on exclusion of individual stations are in Table S1. These criteria excluded PM_{10} and $PM_{2.5}$ from two stations (G3-B, G3-C); and PM_{10} from one station (G3-H). Data points that were below instrument detection limits were set to 0 $\mu g/m^3$ in our analysis. See Table S1 for the instrument detection limits of each instrument.

The eruption period was defined as 19 March 2021 20:00 – 19 September 2021 00:00 UTC in agreement with Barsotti et al., (2023). The background period was defined differently for SO_2 and PM. For SO_2, the background period was defined as 19/03/2020 00:00 - 19/03/2021 19:00 UTC, i.e. one full calendar year before the eruption. Outside of volcanic eruption periods, SO_2 concentrations are generally low with little variability in the Icelandic atmosphere due to the absence of other sources, as shown by previous work (Carlsen et al., 2021a; Ilyinskaya et al., 2017), and subsequently confirmed by this study. The only exception is in the vicinity of aluminium smelters where relatively small pollution episodes occur periodically. A one-year long period was therefore considered as representative of the background SO_2 fluctuations. We checked our background dataset against a previously published study in Iceland that used the same methods (Ilyinskaya et al., 2017) and found no statistically significant difference.

PM background concentrations in Iceland are much higher and more variable than those of SO_2. PM frequently reaches high levels in urban and rural areas, with significant seasonal variations (Carlsen and Thorsteinsson, 2021); the causes of this variability are discussed in the Results and Discussion. To account for this variability, we downloaded PM data for as many non-eruptive years as records existed, and analysed only the period 19 March 20:00 – 19 September 00:00 UTC in each year, i.e. the period corresponding to the calendar dates of the 2021 eruption. From here on, we refer to this period as 'annual period'.

The annual periods in 2010, 2011, 2014, and 2015 were partially or entirely excluded from the non-eruptive background analysis due to eruptions in other Icelandic volcanic systems (Eyjafjallajökull 2010, Grímsvötn 2011, Holuhraun 2014-2015) and associated post-eruptive emissions and/or ash resuspension events. The annual period of 2022, i.e. the year following the 2021 eruption, was partially included in the background analysis: measurements between 19 March 2022 and 1 August 2022 were included, but measurements from 2 August 2022 onwards were excluded because another eruptive episode started in the Fagradalsfjall volcanic system on that date. Since August 2022 there have been nine more eruptions in the same area at intervals of weeks-to-months, and therefore we have not included more recent non-eruptive background data. Although the 2022 annual period is only partially complete, it was particularly important for statistical analysis of PM_1 as operational measurements of this pollutant began only in 2020. The number of available background annual periods for PM_{10} and $PM_{2.5}$ varied depending on when each station was set up, ranging from 1 and 12 stations with an average of 6 (Table S1).

We considered whether the year 2020 had lower PM_{10} and $PM_{2.5}$ concentrations compared to other non-eruptive years due to COVID-19 societal restrictions and the extent to which this was likely to impact our results. The societal restrictions in Iceland were relatively light, for example, schools and nurseries remained open throughout. We found that the average 2020 PM_{10} and $PM_{2.5}$ concentrations fell within the maximum-minimum range of the pre-pandemic years for all stations except at G3-E where PM_{10} was 10% lower than minimum pre-pandemic annual average, and $PM_{2.5}$ was 12% lower; and at G5-A where $PM_{2.5}$ was 25% lower (no difference in PM_{10}). G3-E is at a major traffic junction in central Reykjavík, and G5-A is on a major commuter route to the capital area. For PM_1, only one station was already operational in 2020 (G3-A); PM_1 concentrations at this station were 20% higher in 2020 compared to 2022 (post-pandemic). We concluded that PM data from 2020 should be included in our analysis but we note the potential impact of pandemic restrictions.

2.4 Data analysis

We organised the air quality stations into geographic clusters to assess air quality by region. The geographic clusters were the immediate vicinity of the eruption site (G1, 0-4 km from the eruption site), the Reykjanes peninsula (G2, 9-20 km), the capital area of Reykjavík (G3, 25-35 km), Southwest Iceland (G4, 45-55 km), Hvalfjörður (G5, 50-55 km), North Iceland (G6-A ~280 km; G6-B and C ~330 km), and East Iceland (G7, ~400 km), Fig. 1. Appendix A, Figs. A2-A8 show SO_2 time series data for each individual station in geographic clusters G1-G7, respectively. Appendix A, Figs. A9-A11 show PM time series data for each individual station in geographic clusters G3, G5 and G6, respectively.

For each station that had data for both the eruption and background periods (SO_2 and PM), two-sample t-tests were applied to test whether the differences in background and eruption averages were statistically significant for the different pollutant species.

In addition to time series analysis, we analysed the frequency and number of events where pollutant concentrations exceeded air quality thresholds. Air quality thresholds are pollutant concentrations averaged over a set time period (usually 60 minutes or 24 hours), which are considered to be acceptable in terms of what is robustly known about the effects of the pollutant on health. An air quality threshold exceedance is an event where the pollutant concentration is higher than that set out in the threshold. Evidence-based air quality thresholds have been defined for SO_2, $PM_{2.5}$ and PM_{10}, but not yet for PM_1, largely due to the paucity of regulatory-grade data on concentrations, dispersion and exposure (World Health Organization, 2021). For SO_2, most countries, including Iceland, use an hourly-mean threshold of 350 $\mu g/m^3$; and the threshold for total number of exceedances in a year is 24 (Icelandic Directive, 2016). We used these thresholds for SO_2 in our study. The air quality thresholds for PM are based on 24-hour averages, as there is currently insufficient evidence base for hourly-mean thresholds. For PM_{10} we used the Icelandic Directive (ID) and World Health Organisation (WHO) daily-mean threshold of 50 $\mu g/m^3$, and for $PM_{2.5}$ we used the WHO daily-mean threshold of 15 $\mu g/m^3$, as no ID threshold is defined. While there are currently no evidence-based air quality thresholds available for PM_1, some countries, including Iceland use selected values to help communicate the air pollutant concentrations and their trends to the public. The EAI uses a 'yellow' threshold for PM_1 at 13 $\mu g/m^3$ when visualising data from the regulatory stations and this value was used here (termed 'EAI threshold').

To meaningfully compare the frequency of air quality threshold exceedance events for PM_{10}, $PM_{2.5}$ and PM_1 between the eruption and the non-eruptive background periods we normalised the number of exceedance events, as explained below. This was done because the eruption covered only one annual period (see the definition of 'annual period' in 2.3) but the number of available background annual periods varied between stations depending on how long they have been operational, ranging between 1 and 12 periods. We normalised by dividing the total number of exceedance events at a given station by the number of annual periods at the same station. For example, for a station where the non-eruptive background was 6 annual periods the total number of exceedance events was divided by 6 to give a normalised annual number of exceedance events. The eruption covered one annual period and therefore did not require dividing. We refer to this as 'normalised number of exceedance events' in the Results and Discussion. Table S1 contains summary statistics for all analysed pollutant means, maximum concentrations, number of air quality threshold exceedances, and number of background annual periods for PM data.

Three regulatory stations within geographic cluster G3 (Reykjavík capital area) measured all three PM size fractions (PM_1, $PM_{2.5}$ and PM_{10}), which allowed us to calculate the relative contribution of different size fractions to the total PM concentration. Since PM size fractions are cumulative, in that PM_{10} contains all particles with diameters ≤10 µm, the size modes were subtracted from one another to determine the relative concentrations of particles in the following categories: particles ≤1 µm in diameter, 1 - 2.5 µm in diameter and 2.5 - 10 µm in diameter. The comparison of size fractions between the eruption and the background was limited by the relatively short PM_1 time series and our results should be reexamined in the future when more non-eruptive measurements have been obtained.

3 Results and discussion

3.1 Eruption-driven increase in PM_1 concentrations relative to PM_{10} and $PM_{2.5}$

Emerging studies of the links between PM_1 and health impacts in urban air pollution have shown that even small increases in the PM_1 proportion within PM_{10} can be associated with increasingly worse outcomes; e.g. liver cancer mortalities in China were found to increase for every 1% increase in the proportion of PM_1 within PM_{10} (Gan et al., 2025). Time series of PM_1, $PM_{2.5}$ and PM_{10} concentrations were collected at three stations in Reykjavík capital (G3-A, G3-D and G3-G, Fig. 1), allowing us to compare the relative contributions of the three size fractions in this area (25-35 km distance from the eruption site). There was a measurable change during the eruption period compared to the background, with an increase in PM_1 mass proportion relative to PM_{10} and $PM_{2.5}$ at all 3 stations (Fig. 2). The proportion of PM_1 mass within PM_{10} increased from 16-24% in the background (standard deviation 7-13%) to 24-32% during the eruption (standard deviation 16-19%); and within $PM_{2.5}$ from approximately 47% in the background to ~60% during the eruption period. The eruption-related increase in the $PM_{2.5}$ proportion within PM_{10} was modest, between 4% and 7% compared to the background.

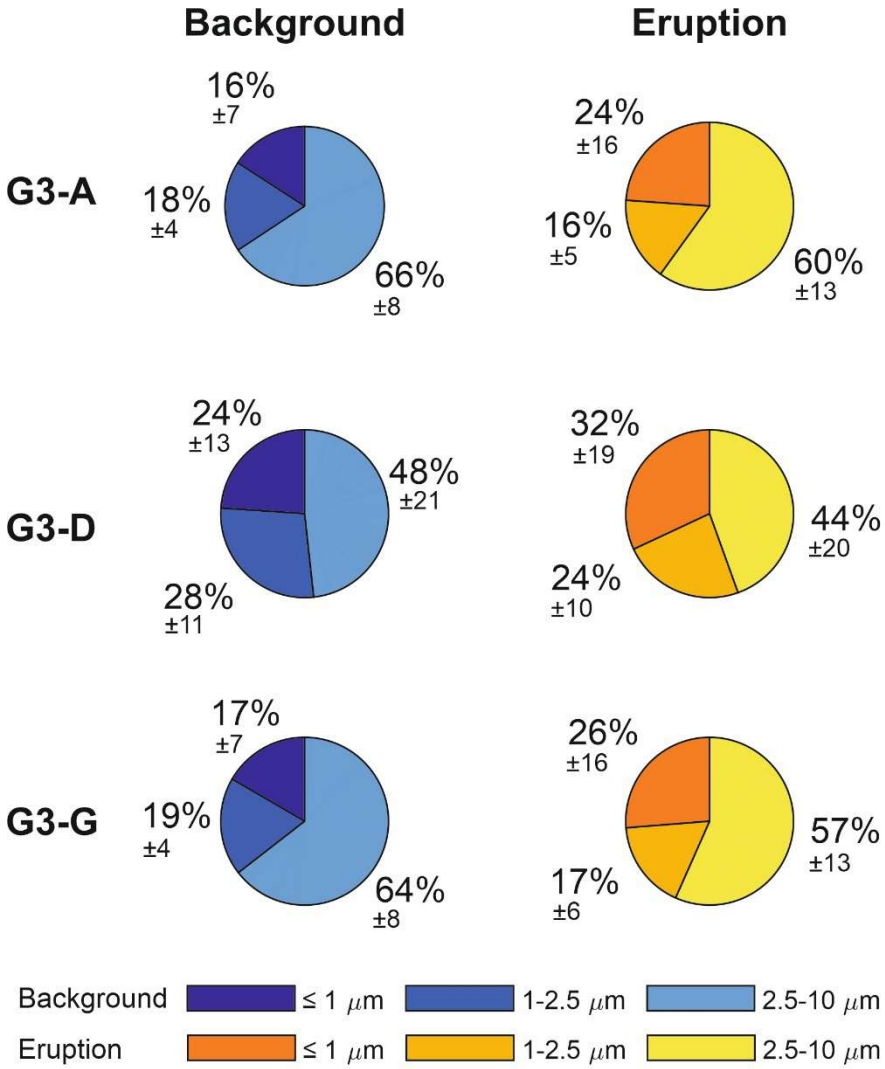

Figure 2: The relative contributions of three PM size fractions within PM_{10} (expressed as mass%) during the non-eruptive background and during the eruption. The size fractions shown are: PM ≤1 µm, PM 1–2.5 µm, and PM 2.5–10 µm in diameter. The %mass is shown as mean ± 1σ standard deviation. G3-A, G3-D and G3-E were the stations in Iceland where all three size fractions were measured, all located within Reykjavík capital area.

These are novel findings showing that volcanic plumes contribute a higher proportion of PM_1 relative to both PM_{10} and $PM_{2.5}$ when sampled at a distal location from the source (25-35 km in this study). When sampled at the active vent, volcanic plumes from basaltic fissure eruptions have been previously shown to contain a large amount of PM_1, but also a substantial proportion of coarse PM (> 2.5 µm) (Ilyinskaya et al., 2017; Martin et al., 2011; Mason et al., 2021). At the vent, the composition of the fine and coarse size modes is typically very different: the finer fraction is primarily formed through the conversion of SO_2 gas into sulphate particles, whereas the coarser fraction consists of fragmented silicate material (i.e. ash), which may be present in small concentrations even in ash-poor fissure eruptions (Ilyinskaya et al., 2021; Mason et al., 2021). The conversion of SO_2

gas to sulphate particles continues for hours to days after emission, generating new fine particles over time (Green et al., 2019; Pattantyus et al., 2018). In contrast, ash particles are not replenished in the plume after emission and are progressively removed through deposition. This may explain the elevated concentrations of particles in the finer size fractions observed downwind of the eruption site relative, to the coarser size fractions. These findings have implications for public health hazards, as volcanic plumes most commonly affect populated areas located tens to hundreds of kilometres from the eruption site.

3.2 Significant but small increases in average pollutant levels

Most areas of Iceland, up to 400 km from the eruption site, recorded a small but statistically significant increase in average SO_2 and PM concentrations during the eruption compared to the background period.

Figure 3 and Table 1 present SO_2 concentrations (hourly-means in $\mu g/m^3$), measured by regulatory stations across Iceland. During the non-eruptive background period, SO_2 concentrations were low (long term average of hourly-means generally <2 $\mu g/m^3$), which is in agreement with previous studies (Ilyinskaya et al., 2017). Stations near aluminium smelters (G5-1 and 2, G6-C, and G7-all) had higher long-term average values and periodically recorded short-lived escalations in SO_2 hourly-mean concentrations of several tens to hundreds $\mu g/m^3$ during the background period (Fig. 3, Table 1 and Table S1). Station G7-D (East Iceland at ~400 km from the eruption site) was the only station where the eruption-related increase in average SO_2 concentrations was below statistical significance. This station was located near an aluminium smelter, and was also missing over one-third of the eruption period data due to technical issues, which may have reduced the observed eruption impact.

The average SO_2 concentrations were higher during the eruption at all of the regulatory stations that had data from both before and during the eruption (n = 16), and the increase was statistically significant ($p < 0.05$) at 15 out of the 16 stations. Across all seven geographic clusters, the absolute increase in average SO_2 concentrations between the background and eruption period was relatively low, on the order of a few $\mu g/m^3$ (Fig. 3 and Table 1). For example, the average concentration across the Reykjavík capital increased from 0.32 $\mu g/m^3$ in the background to 4.1 $\mu g/m^3$ during the eruption.

325

Table 1: SO_2 concentrations (hourly-mean, µg/m^3) in populated areas around Iceland during both the non-eruptive background and the Fagradalsfjall 2021 eruption. 'Average' is the long-term mean of all stations within a geographic area ± 1σ standard deviation. 'Peak' is the maximum hourly-mean recorded by an individual station within the geographic area. 'ID exceedances': the number of times that the SO_2 concentrations exceeded the Icelandic Directive (ID) air quality threshold of 350 µg/m^3. The number of AQ exceedances is the maximum number of exceedances recorded by an individual station within a geographic area.

			SO_2 hourly-mean (µg/m^3)				**ID exceedances (max *n*)**	
Geographic area	**N of stations**	**Distance from eruption site (km)**	**Background average ± standard deviation (1σ)**	**Eruption average ± standard deviation (1σ)**	**Background peak**	**Eruption peak**	**Background**	**Eruption**
Reykjanes peninsula (G2)	6	9-20	0.13±0.45	4.8±44	7.7	2400	0	31
Reykjavík capital (G3)	6	25-35	0.32±1.8	4.1±21	57	750	0	9
South Iceland (G4)	2	45-55	No data	6.1±44	No data	2400	No data	18
Hvalfjörður (G5)	3	50-55	3.9±16	8.2±28	210	860	0	6
North Iceland (G6)	3	280-330	0.41±1.6	1.7±6.3	9.1 at 280 km; 62 at 330 km	250 at 280 km; 48 at 330 km	0	0

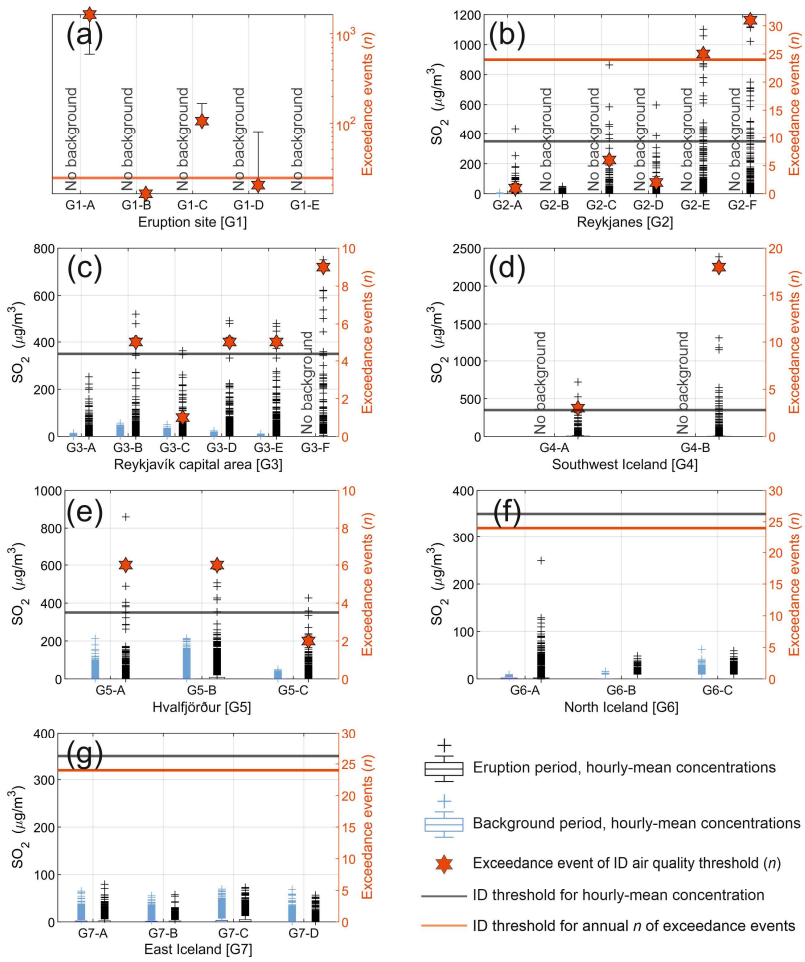

Figure 3: SO_2 hourly-mean concentrations (μg/m³) and number of ID threshold exceedance events, measured by 29 stations across seven geographical areas in Iceland (panels a-g). Pre-eruptive background data are shown for stations that were operational before the eruption began. The data are presented as box-and-whisker plots: boxes represent the interquartile range (IQR), the whiskers extend to +/–2.7σ from the mean, and crosses represent very high values (statistical outliers beyond +/–2.7σ from the mean). Note that the IQR is very low in most cases due to the negligible SO_2 concentrations in the clean local background; as a result, most of the SO_2 pollution episodes are statistical outliers. The ID air quality threshold of 350 μg/m³ (hourly-mean) is indicated by a black horizontal line in all panels. Red stars represent the number of times this threshold was exceeded at each station ('exceedance events'). The annual limit for cumulative hourly exceedance events is 24, shown by an orange horizontal line. Stations with red stars above the orange line exceeded the annual threshold. Panel (a) displays eruption-site measurements collected by LCS, for which only the number of exceedances of the ID air quality threshold (350 μg/m³) is reported. Note the logarithmic scale used in panel (a). Panels (b–g) show data from regulatory stations in populated areas, including SO_2 hourly mean concentrations and the number of exceedance events. Time series plots for each station are available in Appendix A.

Table 2 and Figs. 4-6 present PM_{10}, $PM_{2.5}$ and PM_1 concentrations (daily-means in μg/m^3) measured in the three geographic areas where regulatory-grade monitoring was available. Table 2 shows that when PM concentrations are averaged across all stations within a geographic area, there appears to be negligible or minimal change in average PM levels between the background and eruption periods. However, when individual stations are considered, small but statistically significant differences can be seen (Figs. 4–6), driven by fine-scale spatial variability in PM concentrations. During the eruption, average PM_1 concentrations were significantly higher at all monitored stations (Fig. 4). $PM_{2.5}$ and PM_{10} concentrations were also significantly higher at approximately half of the monitored stations (Figs. 4-6). At these stations, average PM_{10} concentrations increased from 9-10 μg/m^3 during the background to 12-13 μg/m^3 during the eruption; average $PM_{2.5}$ rose from 3-4 μg/m^3 to ~5 μg/m^3; and average PM_1 increased from 1.3-1.5 μg/m^3 to ~3 μg/m^3 (Fig. 4).

The locations that recorded statistically significant eruption-related increases in average PM_{10} and $PM_{2.5}$ concentrations generally had lower non-eruptive background levels. The stations with higher background PM_{10} and $PM_{2.5}$ were generally situated near roads with heavy traffic. This suggests that local sources, such as road traffic, were more important sources of PM_{10} and $PM_{2.5}$ than the distal eruption. However, the eruption's impact on PM_{10} and $PM_{2.5}$ was more noticeable in areas with lower background concentrations. Average levels of PM_1 were unequivocally higher during the eruption period compared to the background, although this pollutant was only monitored in the Reykjavík capital area. It remains to be investigated whether volcanic contribution to PM_1 would also dominate over other sources in more distal communities.

Table 2 PM_{10}, $PM_{2.5}$ and PM_1 concentrations (μg/m^3, 24-h mean) in populated areas around Iceland during both the non-eruptive background ('B/G') and the Fagradalsfjall 2021 eruption ('Eruption'). 'Average' refers to the long-term mean of 24-hour values of all stations within a geographic area ± 1σ standard deviation. 'Peak' is the maximum 24 h-mean recorded by an individual station within the geographic area. 'AQ exceedances' denotes the number of times PM concentrations exceeded the following thresholds: PM_{10} - 50 μg/m^3; $PM_{2.5}$ - 15 μg/m^3; PM_1 - 13 μg/m^3. The 'AQ exceedances' value is the maximum number of exceedances recorded by any single station within a geographic area.

			PM_{10}						$PM_{2.5}$						PM_1					
			Average (24-h mean ± 1σ, μg/m^3)		Peak (24-h mean, μg/m^3)		AQ exceedances (max *n*)		Average (24-h mean ± 1σ, μg/m^3)		Peak (24-h mean, μg/m^3)		AQ exceedances (max *n*)		Average (24-h mean ± 1σ, μg/m^3)		Peak (24-h mean, μg/m^3)		AQ exceedances (max *n*)	
Geographic area	*n* of stations (PM_{10}, $PM_{2.5}$, PM_1)	Distance from eruption site (km)	B/G	Eruption	B/G	Eruption	B/G	Eruption	B/G	Eruption	B/G	Eruption	B/G	Eruption	B/G	Eruption	B/G	Eruption	B/G	Eruption
Reykjavík capital (G3)	5, 4, 3	25-35	15±11	14±14	170	140	2.9	5	6.6±6.8	5.7±6.2	87	48	15	22	1.4±0.94	2.8±2.6	6.3	20	0	4
Hvalfjörður (G5)	3	50-55	5.6±5.7	7.3±7.8	58	59	0.25	2	2.1±3.4	3.9±5.3	34	31	1	8	No data					
North Iceland (G6)	3	280-330	7.7±10	8.9±11	100	79	7.7	7	0.53±1.9	0.71±2.2	13	16	0	1						

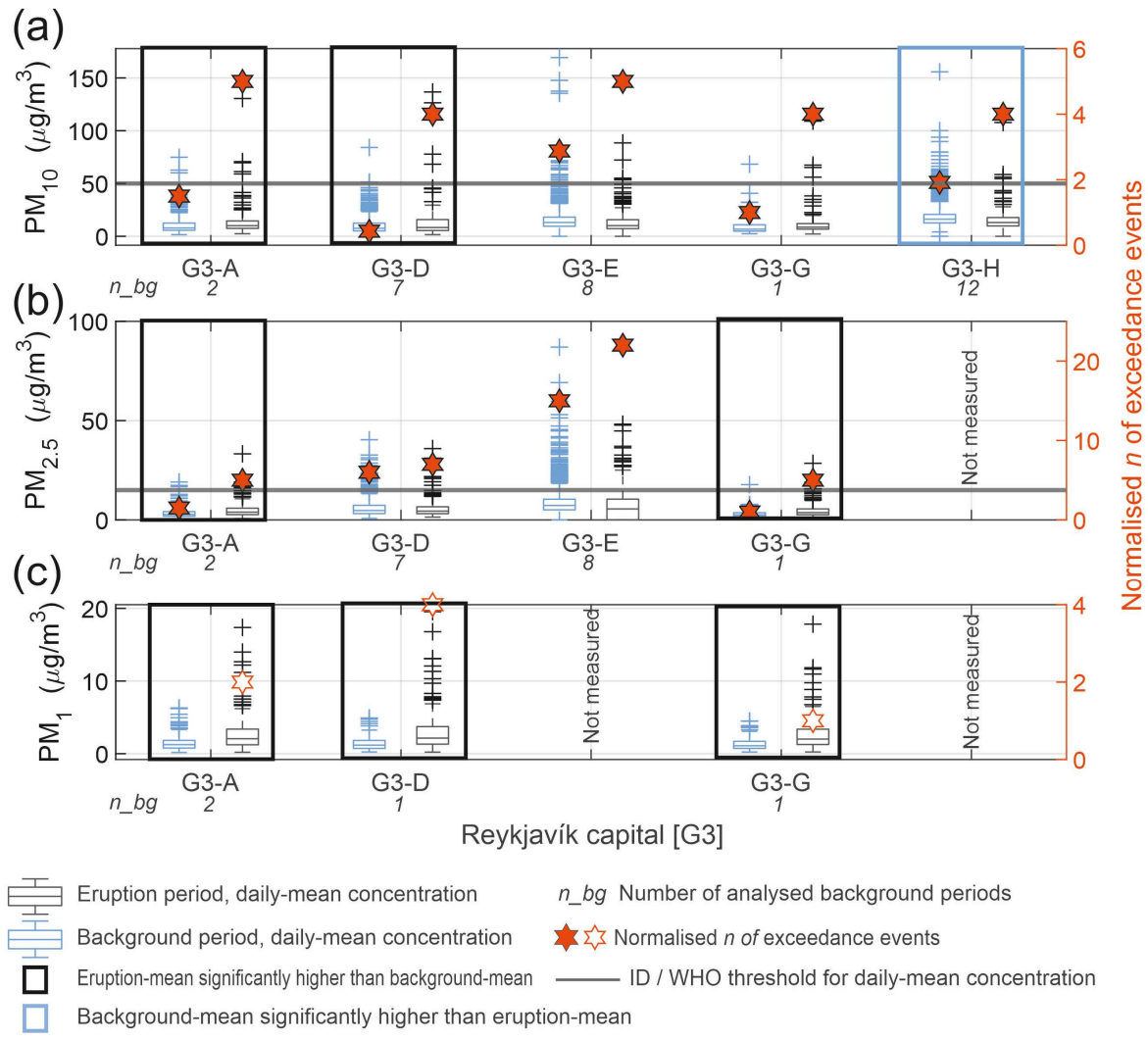

Figure 4: Daily-mean concentrations of (a) PM_{10}, (b) $PM_{2.5}$, and (c) PM_1 (μg/m³) measured in the Reykjavík capital area. The data are presented as box-and-whisker plots, where boxes represent the interquartile range (IQR), the whiskers extend to +/–2.7σ from the mean, and crosses represent very high values (statistical outliers beyond +/–2.7σ from the mean). The median is shown with a horizontal line within each box. Pre-eruptive background data are shown for stations that were operational before the eruption started. The value *n_bg* shown on the x-axis indicates the number of background annual periods available for each station (see Methods for the definition of a background annual period). Stations where the average concentration during the eruption period was significantly higher ($p < 0.05$) than during the background are highlighted with a black box. Stations where the average concentration during the eruption was significantly lower than during the background are highlighted with a blue box. The absence of a box indicates no significant difference between the eruption and background periods. Stars with solid orange fill represent the normalised number of times PM_{10} and $PM_{2.5}$ concentrations at each station exceeded the Icelandic Directive (ID) air quality thresholds of 50 μg/m³ and 15 μg/m³ (24-hour mean), respectively. For PM_1, non-filled stars indicate the number of times concentrations during the eruption exceeded the Environmental Agency of Iceland (EAI) threshold of 13 μg/m³(24-hour mean). Different symbols (filled vs. non-filled stars) are used to distinguish between internationally accepted, evidence-based ID thresholds (PM_{10} and $PM_{2.5}$) and the locally applied EAI threshold for PM_1, which is not internationally standardized. The number of threshold exceedance events is normalized to the length of the measurement period—refer to the main text for details on the normalization method. Time series plots for each station are available in Appendix A.

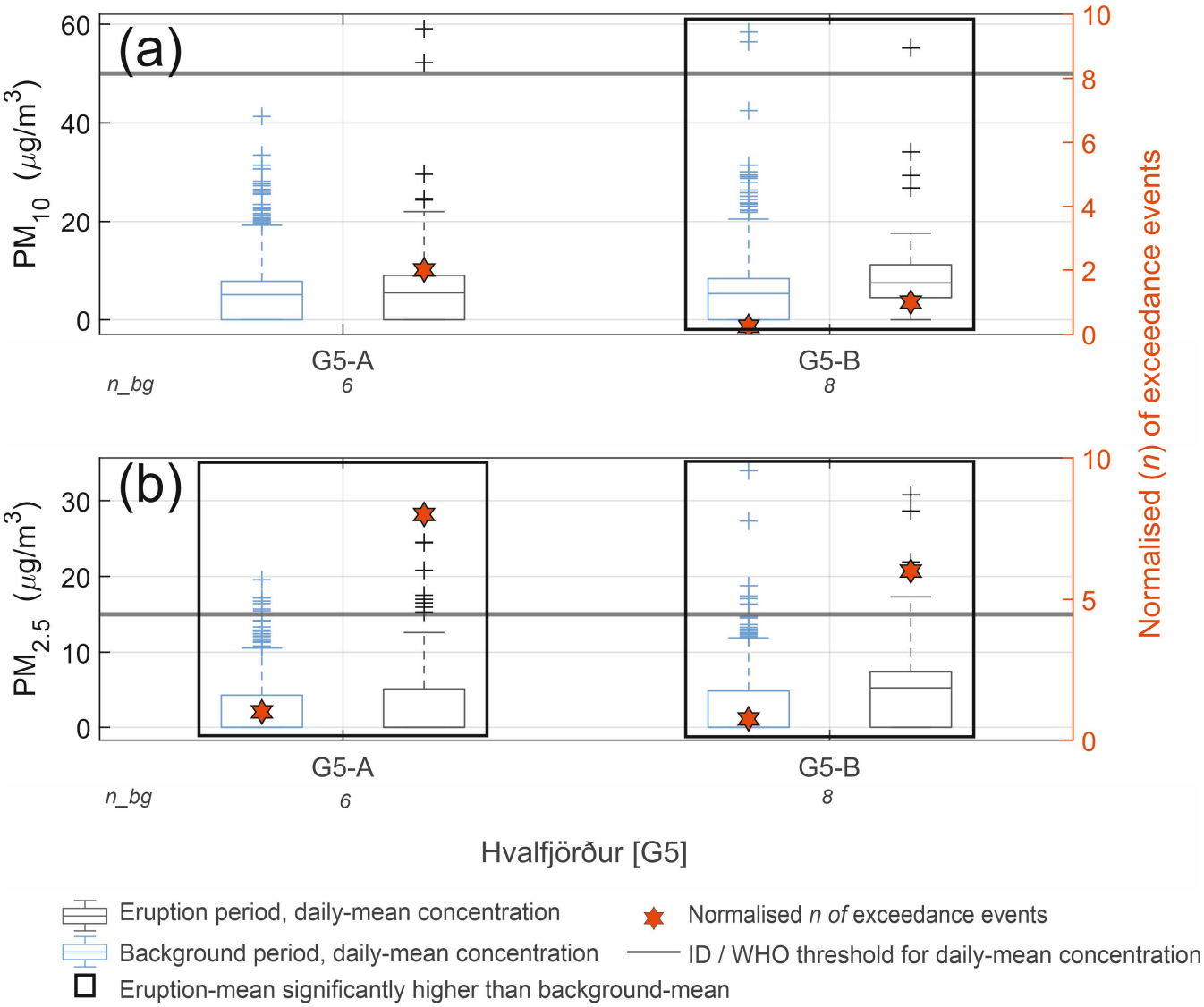

Figure 5: Daily-mean concentrations of (a) PM_{10}, and (b) $PM_{2.5}$ (µg/m³), measured in the Hvalfjörður area. The data are presented as box-and-whisker plots, where boxes represent the interquartile range (IQR), the whiskers extend to +/–2.7σ from the mean, and crosses represent very high values (statistical outliers beyond +/–2.7σ from the mean). The median is shown as a horizontal line within each box; if the median line is absent, the value is zero. Pre-eruptive background data are shown for stations that were operational before the eruption started. The value *n_bg* shown on the x-axis indicates the number of background annual periods available for each station (see Methods for the definition of a background annual period). Stations where the average concentration during the eruption period was significantly higher (p <0.05) than during the background are highlighted with a black box. The absence of a box indicates no significant difference. Stars with solid orange fill show the normalized number of times PM_{10} and $PM_{2.5}$ concentrations at each station exceeded the Icelandic Directive (ID) air quality thresholds of 50 µg/m³ and 15 µg/m³ (24-hour mean), respectively. The number of threshold exceedance events is normalized to the length of the measurement period—refer to the main text for details on the normalization method. Time series plots for each station are available in Appendix A.

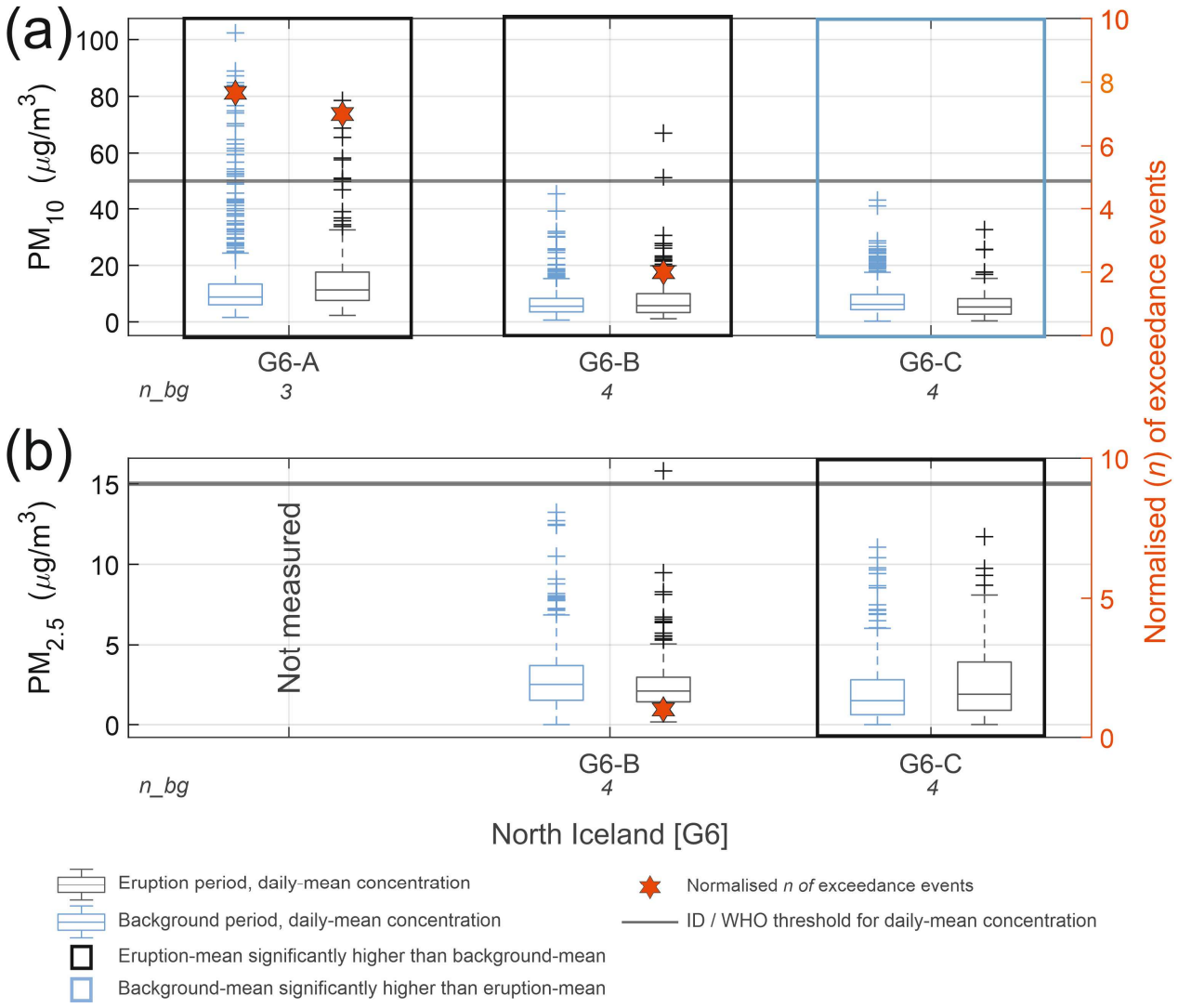

Figure 6: Daily-mean concentrations of (a) PM_{10}, and (b) $PM_{2.5}$ ($\mu g/m^3$), measured in North Iceland. The data are presented as box-and-whisker plots, where boxes represent the interquartile range (IQR), the whiskers extend to +/–2.7σ from the mean, and crosses represent very high values (statistical outliers beyond +/–2.7σ from the mean). The median is shown as a horizontal line within each box; if the median line is absent, the value is zero. Pre-eruptive background data are shown for stations that were operational before the eruption started. The value *n_bg* shown on the x-axis indicates the number of background annual periods available for each station (see Methods for the definition of a background annual period). Stations where the average concentration during the eruption period was significantly higher ($p < 0.05$) than during the background are highlighted with a black box. Stations where the average concentration during the eruption was significantly lower than during the background are highlighted with a blue box. The absence of a box indicates no significant difference. Stars with solid orange fill show the normalized number of times PM_{10} and $PM_{2.5}$ concentrations at each station exceeded the Icelandic Directive (ID) air quality thresholds of 50 $\mu g/m^3$ and 15 $\mu g/m^3$ (24-hour mean), respectively. The number of threshold exceedance events is normalized to the length of the measurement period—refer to the main text for details on the normalization method. Time series plots for each station are available in Appendix A.

3.3 Impact on pollutant peak concentrations and number of air quality exceedance events

Unlike the modest—or in some cases negligible—increases in average concentrations of PM and SO_2, the eruption was associated with substantial increases in the number of air quality threshold exceedance events in both near-field and far-field locations.

Figure 3 and Table 1 compare the background and eruption periods in terms of peak SO_2 concentrations and the number of exceedance events relative to the Icelandic Directive (ID) air quality threshold of 350 µg/m³ (hourly-mean). During the non-eruptive background period, SO_2 concentrations did not exceed the ID threshold at any station. In contrast, during the eruption, the number of exceedance events ranged from 0 to 31 at individual stations, and were, in broad terms, highest closer to the eruption site (Fig. 3 and Table 1). The ID threshold for total annual hourly-mean exceedances (n = 24) was exceeded in the geographic cluster immediately adjacent to the eruption site (G1), where up to 1,600 exceedance events were recorded at an individual station. Additionally, two communities on the Reykjanes Peninsula (G2) recorded 25 and 31 exceedance events, respectively. We attribute the combination of a relatively low absolute increase in average SO_2 concentrations and a large increase in peak concentrations to a combination of the dynamic nature of the eruption emissions (Barsotti et al., 2023; Pfeffer et al., 2024) and highly variable local meteorological conditions (wind rose for the eruption site in Fig. A12). These factors resulted in the volcanic plume being intermittently advected into populated areas, rather than acting as a continuous source of pollution.

PM_1 concentrations did not exceed the EAI threshold of 13 µg/m³ during the background period. However, during the eruption, exceedances occurred between three and five times at all stations where PM_1 was monitored (Fig. 4, Table 2). The number of PM_{10} and $PM_{2.5}$ exceedance events was also higher during the eruption period at all stations in the Reykjavík capital area (G3) and in Hvalfjörður (G5), as well as at two out of three stations in North Iceland (G6) that recorded any threshold exceedances. Peak PM_1 concentrations (daily-mean) increased from 5–6 µg/m³ during the background period to approximately 20 µg/m³ during the eruption period across all three monitoring stations in the Reykjavík capital area (G3). The volcanic impact on PM_{10} and $PM_{2.5}$ was more variable. Stations in the Reykjavík capital area with cleaner PM_{10} and $PM_{2.5}$ backgrounds (defined here as peak daily-mean below 80 µg/m³ for PM_{10} and below 20 µg/m³ for $PM_{2.5}$) showed larger eruption-related impacts than stations with more polluted background conditions (peak daily-means ≥110 µg/m³ for PM_{10} and ≥40 µg/m³ for $PM_{2.5}$). At the cleaner stations, peak daily-mean concentrations increased by up to 40–60 µg/m³ for PM_{10} and by 10–14 µg/m³ for $PM_{2.5}$ during the eruption. In contrast, the more polluted stations did not exhibit noticeable increases in peak PM_{10} or $PM_{2.5}$ concentrations. Further afield, in Hvalfjörður and North Iceland (Figures 5–6), the number of monitoring stations was too low for statistical analysis. However, a similar pattern was observed: stations with lower non-eruptive background PM_{10} and $PM_{2.5}$ levels generally recorded increases in peak daily mean concentrations of up to ~20 µg/m³ and ~5 µg/m³, respectively, above background levels.

The statistically significant impact on both average and peak PM levels observed in the Reykjavík capital area and as far as 300 km from the eruption site is remarkable, given the relatively small size of the eruption and the prominence of non-volcanic

PM sources in Iceland. In rural regions, the primary non-volcanic source of PM is resuspended natural dust from highland deserts, with elevated levels typically occurring during the drier summer months (Butwin et al., 2019). In urban areas, non-volcanic PM pollution peaks are generally higher in winter, primarily due to tarmac erosion caused by studded tyres (Carlsen and Thorsteinsson, 2021). The unequivocal eruption-related increase in average and peak concentrations of PM_1 suggests that volcanic fissure eruptions are one of, or potentially the most, important source of PM_1 in Iceland. Table 3 compares concentration ratios of the three measured PM size fractions in Reykjavík across three scenarios: a representative eruption-free background period, the 2021 volcanic plume, and two Icelandic desert dust storms in 2023. Our analysis is based only on summer conditions because of the timing of the 2021 eruption. During winter, contributions from tarmac erosion due to studded tyres may influence these ratios, and short-lived peak concentrations may also occur during New Year's Eve fireworks. Data from winter-time eruptions are needed to better understand seasonal variability in PM_1 source contributions.

Although based on a limited dataset, our comparison suggests distinct 'fingerprint' ratios for the different pollution sources (Table 3). These ratios may be useful for identifying the sources of PM pollution episodes in Reykjavík and potentially in other distal populated areas, especially when source attribution is challenging using meteorological or visual observations.

Table 3. Concentration ratios of PM size fractions (hourly-means, µg/m³) associated with different pollution sources in the Reykjavík capital area. Rows 1 and 2 represent periods considered typical of Reykjavík background conditions: the 'Summer period', when studded tyres are not in use (banned between April and November), and a period during the 2021 eruption when the volcanic plume was advected away from Reykjavík. Rows 3–6 show ratios during the 2021 eruption when the plume was advected toward Reykjavík. For definitions of 'fresh' and 'mature' plume, see Section 3.4. Rows 7 and 8, labelled 'Desert dust', correspond to pollution episodes caused by Icelandic highland desert storms (source area ~200 km from Reykjavík), confirmed by meteorological and visual observations from the Icelandic Meteorological Office (IMO). Station G3-G is listed first, as it is considered the most sensitive to the presence of volcanic plume due to its low background concentrations from local sources.

					G3-G	G3-A	G3-D	G3-G	G3-A	G3-D	G3-G	G3-A	G3-D
	Start date	Start time	End date	End time	PM_1/PM_{10}	PM_1/PM_{10}	PM_1/PM_{10}	$PM_1/PM_{2.5}$	$PM_1/PM_{2.5}$	$PM_1/PM_{2.5}$	$PM_{2.5}/PM_{10}$	$PM_{2.5}/PM_{10}$	$PM_{2.5}/PM_{10}$
Summer period, no eruption	01/05/2020	00:00	01/09/2020	00:00	0.16	0.15	0.13	0.44	0.43	0.22	0.35	0.34	0.61
Eruption but no plume in Reykjavík	01/04/2021	09:00	02/04/2021	10:00	0.17	0.19	0.24	0.41	0.43	0.45	0.42	0.43	0.54
Fresh plume	18/07/2021	10:00	19/07/2021	16:00	0.65	0.68	0.7	0.9	0.92	0.84	0.72	0.73	0.78
Mature plume 1	28/04/2021	08:00	29/04/2021	20:00	0.43	0.29	0.49	0.8	0.73	0.8	0.53	0.39	0.6
Mature plume 2	19/05/2021	14:00	21/05/2021	11:00	0.71	0.65	0.85	0.96	0.95	0.95	0.73	0.68	0.89
Mature plume 3	01/07/2021	09:00	06/07/2021	08:00	0.67	0.59	0.65	0.91	0.88	0.84	0.74	0.66	0.74
Desert dust 1	03/11/2023	13:00	04/11/2023	02:00	0.02	n/a	0.02	0.11	n/a	0.13	0.15	n/a	0.15
Desert dust 2	08/11/2023	14:00	09/11/2023	00:00	0.01	n/a	0.01	0.1	n/a	0.086	0.15	n/a	0.15

3.4 Fine-scale temporal and spatial variability in SO_2 and PM_1 peaks

The dense regulatory monitoring network located 9–35 km from the eruption site (clusters G2 and G3) revealed fine-scale variability in SO_2 concentrations at these relatively distal locations. Five out of six stations on the Reykjanes peninsula (monitoring SO_2 only) were positioned north and northwest of the eruption site, within the most common wind direction (Figure A12). Despite being only 3–16 km apart, two of these stations—G2-E and G2-F—recorded 25 and 31 hourly SO_2 exceedance events, respectively, while G2-B, G2-C, and G2-D recorded between 0 and 6 events (Fig. 3). To ensure this pattern was not an artifact of staggered station deployment, we recalculated exceedance events starting from 7 May 2021, the date by which all G2 stations were operational. The results remained consistent: G2-E and G2-F recorded 7 and 26 events, respectively, while G2-B, G2-C, and G2-D recorded between 0 and 6 events. The spatio-temporal difference between the two 'high-exceedance' stations—G2-E and G2-F, located within 5 km of each other—is also noteworthy. During the first seven weeks of the eruption (19 March – 7 May 2021), G2-E recorded 18 of its 25 total exceedance events, while G2-F recorded only 5 of its 31. Figure 7 illustrates one such episode of fine-scale variability in SO_2 concentrations between G2 stations (28–30 May 2021). During this event, the volcanic pollution cloud 'migrated' between the closely spaced stations G2-C, G2-D, and G2-E (separated by ~2 km). The plume first reached G2-C, then shifted to G2-D and G2-E, with G2-D recording nearly twice the peak concentration of G2-E. This demonstrates that the edges of the volcanic pollution cloud at ground level were sharply defined. The movement and sharp boundaries of the plume during the 28–30 May episode are shown in an animation in Supplementary Figure S1, based on a dispersion model used operationally for volcanic air quality advisories during the eruption by the IMO (Barsotti, 2020; Pfeffer et al., 2024). The model results are used here for qualitative purposes—as a binary yes/no indicator of potential plume presence at ground level. This is because the model has been shown to have a reasonable skill in predicting the general plume direction but relatively low accuracy in simulating ground-level SO_2 concentrations for the 2021 eruption (Pfeffer et al., 2024).

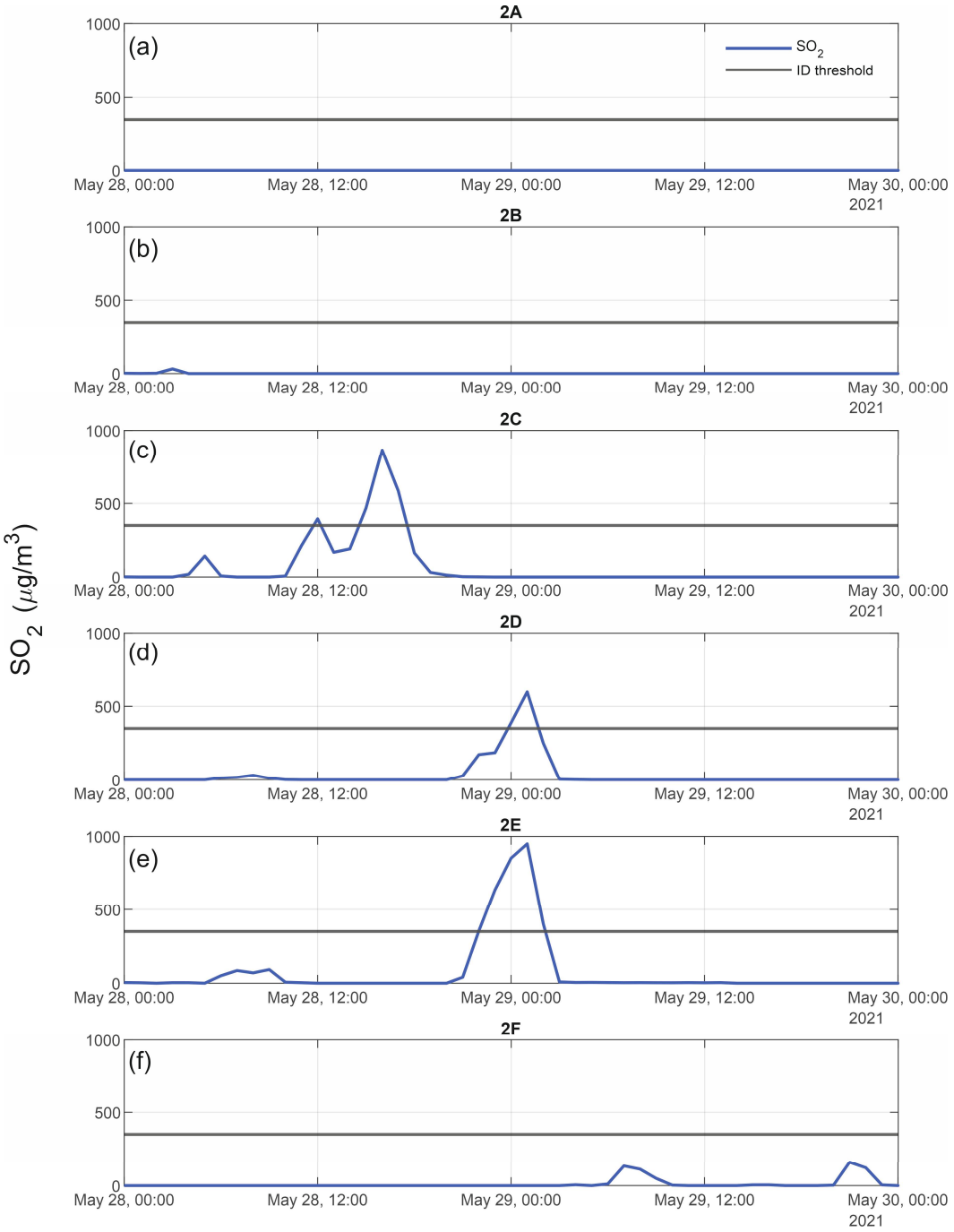

495 **Figure 7: Spatial and temporal variability in SO_2 concentrations (µg/m³, hourly-mean) between monitoring stations on the Reykjanes peninsula (G2) during 28–30 May 2021. The Icelandic Directive (ID) air quality threshold for hourly SO_2 concentrations (350 µg/m³) is indicated by a black horizontal line. Panel (a): Station G2-A. Panel (b): Station G2-B. Panel (c): Station G2-C. Panel (d): Station G2-D. Panel (e): Station G2-E. Panel (f): Station G2-F. The map of the stations' locations is on Fig. 1.**

Stations in the Reykjavík capital area (G3), located 25–35 km from the eruption site and within <1–10 km of one another (Fig. 1), recorded fine-scale variability in pollutant concentrations—even at this relatively large distance from the source. The most significant volcanic plume advection episode occurred on 18–19 July 2021, during which the G3 stations cumulatively recorded 21 SO_2 hourly mean air quality exceedance events—out of the 23 total exceedances recorded throughout the entire eruption. This episode revealed pronounced spatio-temporal variability in volcanic pollutant concentrations. Figure 8 illustrates the variation in SO_2 and PM_1 abundances during this episode, shown as time series (Figs. 8a–8b) and as concentration ratios (Figs. 8c–8d). This discussion focuses on PM_1 rather than $PM_{2.5}$ and PM_{10} because PM_1 was more pronounced in the volcanic air pollution, as discussed in Section 3.1 and shown in Figs. 8c–8d. Both SO_2 and PM_1 were significantly elevated above background levels at all G3 stations during the advection episode. Stations G3-A and G3-E, located within 1 km of each other, showed notable differences: G3-E recorded a maximum SO_2 concentration of 480 µg/m³ and five exceedance events, while G3-A recorded a peak of 250 µg/m³ and no exceedances (Figs. 3 and 8a). Similar fine-scale differences were observed in PM_1: for example, G3-D recorded up to twice the PM_1 hourly mean concentrations of G3-G during the same episode (Fig. 8b). Topographic elevation differences are unlikely to explain this spatial variability, as most G3 stations are located between 10 and 40 m above sea level (a.s.l.), with G3-F at 85 m a.s.l. One potential contributing factor could be the channelling or downwash of air currents by urban buildings—a process that may be particularly relevant in central Reykjavík. This warrants further investigation, such as through fine-scale dispersion modelling, but is beyond the scope of this study. Supplementary Figure S2 shows an animation of the simulated dispersion of volcanic SO_2 at ground level during the 18–19 July episode as simulated by the IMO model (Pfeffer et al., 2024). As discussed by Pfeffer et al. (2024), the dispersion model did not accurately simulate all ground-level pollution events, including this one—the largest SO_2 pollution episode in Reykjavík during the eruption. This highlights the challenges of accurately simulating ground-level dispersion of volcanic emissions from eruptions like Fagradalsfjall 2021, as well as other small but highly dynamic natural and anthropogenic sources (Barsotti, 2020; Pfeffer et al., 2024; Sokhi et al., 2022). High-resolution observational datasets, including those presented here, can support improvements in dispersion model performance.

The relative proportions of SO_2 and PM_1 during the 18–19 July advection episode varied strongly between the two stations that measured both pollutants (G3-A and G3-D). The peak hourly mean SO_2 concentration differed by nearly a factor of two between the stations (Fig. 8a), whereas peak PM_1 hourly means differed by no more than 20% (Fig. 8b). During the advection episode, both pollutants exhibited three principal concentration peaks. The first peak, on 18 July at 13:00, corresponded to the highest SO_2 concentration recorded at station G3-D. The final peak, on 19 July at 23:00, marked the highest PM_1 concentration at the same station (Figs. 8a–8b).

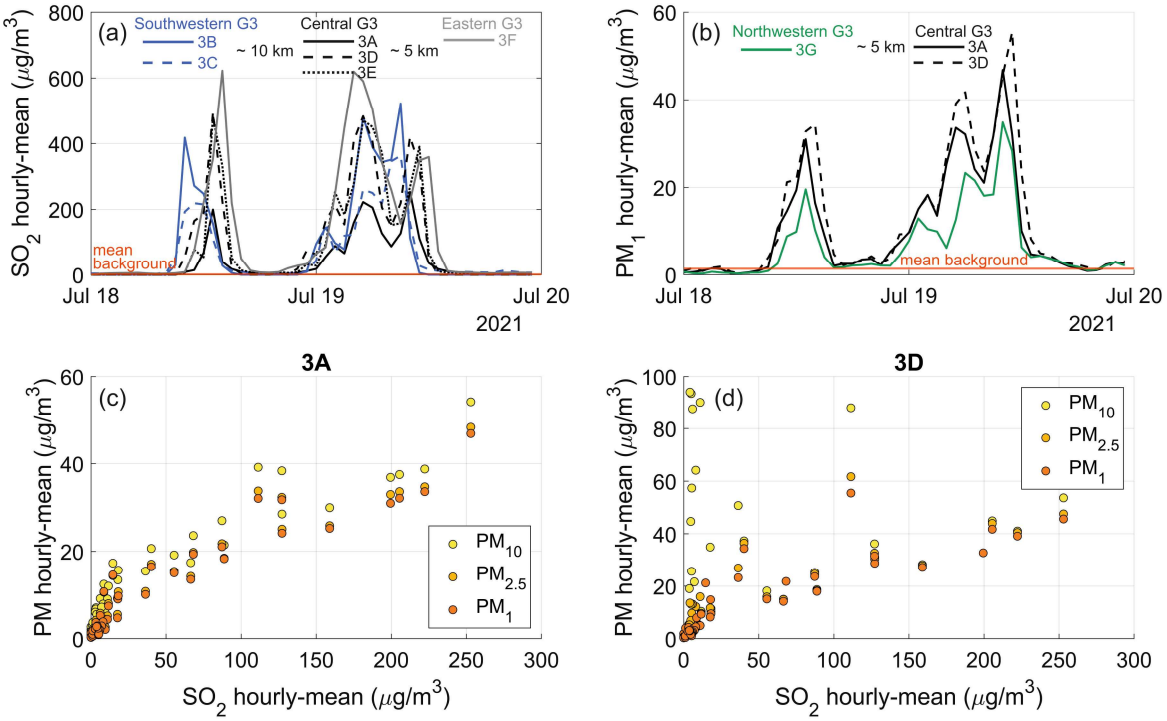

Figure 8: SO_2 and PM concentrations (µg/m^3, hourly-mean) during a 'fresh' volcanic plume advection episode in the Reykjavík capital area (G3) on 18–19 July 2021. Stations G3-A to G3-F are regulatory monitoring sites, and the figure indicates their respective locations within Reykjavík (southwestern, central, eastern, and northwestern), along with approximate distances between them. Panel (a): SO_2 hourly-mean time series. Panel (b): PM_1 hourly-mean time series. Panel (c): Scatter plot of concentrations of SO_2 and PM_{10}, $PM_{2.5}$ and PM_1 at station 3A, which measured all four pollutants. Panel (d): Scatter plot of concentrations of SO_2 and PM_{10}, $PM_{2.5}$ and PM_1 at station 3D, which measured all four pollutants.

We also examined fluctuations in SO_2 and PM_1 during an advection episode of a chemically mature volcanic plume—locally known as *móða* (or *vog* in English, meaning volcanic smog)—in the Reykjavík capital area between 1 and 7 July 2021 (Figs. 9a–9d). A chemically mature plume has undergone significant gas-to-particle conversion of sulfur in the atmosphere and, as shown by Ilyinskaya et al. (2017), may be advected into populated areas several days after the initial emission. Compared to a fresh plume (Figs. 8c–8d), the mature plume (Figs. 9c–9d) is characterized by a higher PM/SO_2 ratio, with SO_2 elevated above background levels to a variable degree—sometimes only slightly (Ilyinskaya et al., 2017). Conditions that typically facilitate the formation and accumulation of *móða* include low wind speeds, high humidity, and intense solar radiation. Based on these factors, the 1–7 July episode was identified by the Icelandic Meteorological Office (IMO) as *móða* at the time of the event, and a public air quality advisory was issued. Figures 9c–9d show that during the *móða* episode, PM_1 was frequently elevated without a correspondingly high increase in SO_2. While SO_2 peaks were well-defined, PM_1 remained consistently elevated above background levels throughout the entire episode, with less prominent individual concentration peaks. This suggests that

PM_1 may ground more persistently than SO_2—an observation that could be tested in future studies using high-resolution dispersion modelling near the surface.

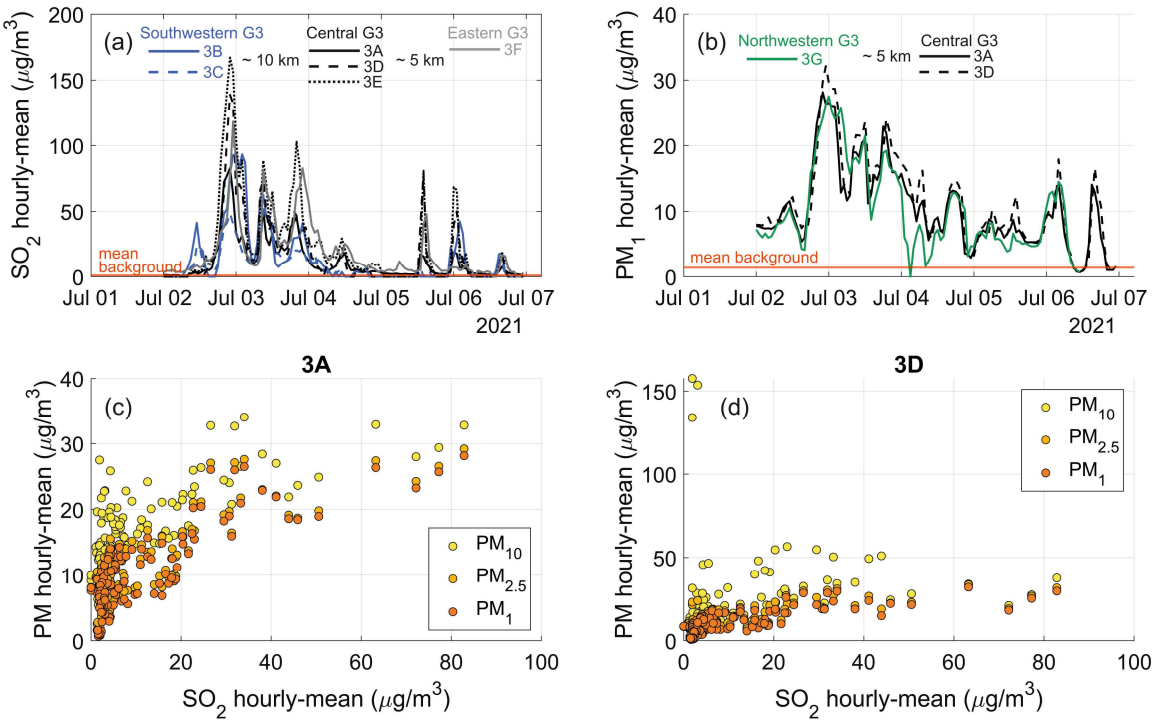

Figure 9: SO_2 and PM concentrations (µg/m3) during a 'mature' volcanic plume advection episode in Reykjavík capital area (G3) 1-7 July 2021. 3A to 3F are names of regulatory stations and the figure indicates their respective locations within Reykjavík (southwestern, central, eastern, and northwestern) and the approximate distance between them. Panel (a): SO_2 hourly-means time series. Panel (b): PM_1 hourly-means time series. Panel (g): Scatter plot between concentrations of SO_2 and PM_{10}, $PM_{2.5}$ and PM_1 at station 3A, which measured all of these pollutants. Panel (h): Scatter plot between concentrations of SO_2 and PM_{10}, $PM_{2.5}$ and PM_1 at station 3D, which measured all of these pollutants.

3.5 Estimates of population exposure and implications for health impacts

3.5.1 Exposure of residents

We assessed the frequency of exposure to SO_2 concentrations above the ID air quality threshold (350 µg/m³ hourly-mean) in populated areas. Based on available evidence in volcanic areas, exceedances of this threshold are associated with adverse health effects (Carlsen et al., 2021a, b). Individuals exposed to elevated concentrations of volcanic SO_2 were also exposed to elevated levels of fine particulate matter, since the volcanic pollution episodes typically contained elevated levels of SO_2, PM_1 and $PM_{2.5}$ —and to a lesser extent, PM_{10} (Figs. 8 and 9). The exceedance of the SO_2 air quality threshold is therefore a proxy for exposure to elevated SO_2 and PM concentrations.

Population data for Iceland in the year 2020 were obtained from Statistics Iceland (2022) and were considered representative for 2021. Data were collected at the municipal level and included both total population and age-specific demographics. Municipality-level population datasets are relatively easy to obtain and are therefore frequently used in population exposure analyses (Caplin et al., 2019), but there are limitations to the resolution due to significant fine-scale spatial variations such as reported in this study.

In 2020, Iceland had a population of 369,000. Of this total, 6% were aged ≤4 years and 15% were aged ≥65 years—age groups which have been shown to be more vulnerable to volcanic air pollution (Carlsen et al., 2021b, a). A total of 263,000 people—equivalent to 71% of the national population—resided within 50 km of the Fagradalsfjall eruption site, where most SO_2 air quality threshold exceedances occurred. Figure 10 presents municipality-level population data for this area, including total population and density, the number and density of individuals in vulnerable age groups, the locations of hospitals, and the number of ID air quality threshold exceedances recorded at monitoring stations.

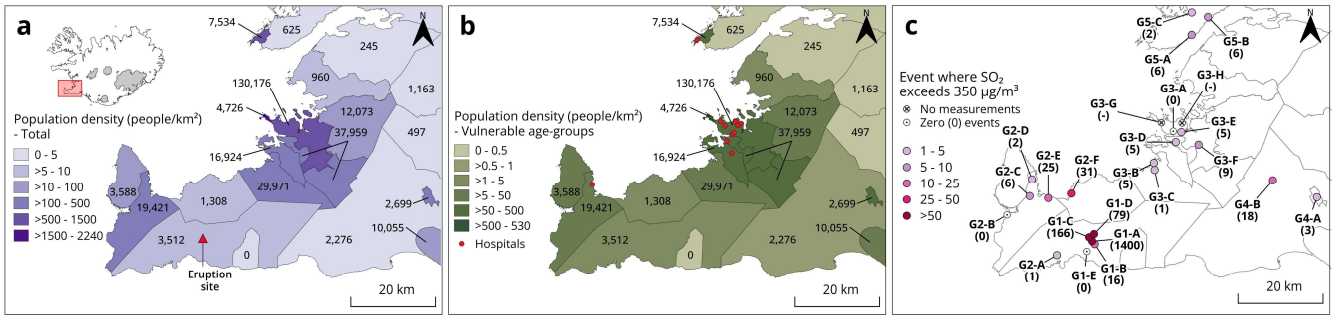

Figure 10: Potential exposure of the residents in the densely populated southwestern part of Iceland, including the Reykjavík capital area (G3) to above-threshold SO_2 concentrations. Population data are from Statistics Iceland for 2020. Panel (a): The number of residents and the population density at the municipality level. The number of residents is shown for each municipality, and the colour scale represents the population density (*n* of people/km² in each municipality). Panel (b): Potentially vulnerable age groups (≤ 4 years and ≥ 65 years of age). The number of people in the vulnerable age groups is shown for each municipality, and the colour scale represents the population density (*n* of people/km² in each municipality). The map also shows the location of hospitals. Panel (c): Number of times when the SO_2 concentrations exceeded the ID air quality threshold of 350 µg/m³ hourly-mean during the eruption period as measured by the regulatory stations in areas G1, G2 and G3. Source and copyright of basemap and cartographic elements: Icelandic Met Office & Icelandic Institute of Natural History

The Reykjavík capital area had approximately 210,000 residents (60% of the total population), a high density of individuals in the potentially more vulnerable age groups, and a large number of hospitals (area G3 on Fig. 10). Air quality stations in this densely populated capital area recorded between 0 and 9 threshold exceedance events during the eruption period. Fine-scale spatial differences in ground-level pollutant concentrations (see Section 3.4) may have played a critical role in determining people's exposure. For example, one of the largest hospitals in the country was located approximately equidistant (~2 km) from stations G3-A and G3-E, which recorded 0 and 5 SO_2 exceedance events, respectively. As a result, it remains unknown how frequently individuals at the hospital were exposed to above-threshold SO_2 levels. Similarly, the hospital closest to the eruption site—located about 20 km away—was situated between two monitoring stations, G2-D and G2-E, which recorded

markedly different numbers of exceedance events: 2 and 25, respectively (Fig. 10). These examples highlight the importance of spatial resolution in air quality monitoring for accurately assessing population exposure.

The most frequent exposure to potentially unhealthy SO_2 levels occurred predominantly within a 20 km radius of the eruption site, particularly in municipalities on the Reykjanes Peninsula. In this area (G2, Fig. 10), up to 31 exceedance events were recorded—surpassing the annual threshold of 24 exceedances (n = 24). However, exposure estimates based solely on place of residence may not fully capture individual exposure, especially for working adults who commute. For example, station G2-A in the township of Grindavík recorded only one exceedance event, yet many residents worked at Keflavík Airport, where higher SO_2 levels were observed (five exceedance events at station G2-C, Fig. 10). Conversely, residents in the town of Vogar (station G2-E, 25 exceedance events) who commuted to the Reykjavík capital area—where fewer exceedances were recorded (0–9 events)—may have experienced lower actual exposure than estimated based on residence alone. In contrast, exposure estimates for children are likely more accurate, as most attend schools within walking distance or a short commute from home. The same applies to long-term hospital inpatients, whose exposure is closely tied to the location of the healthcare facility.

From a nationwide public health perspective, it was fortunate that volcanic pollutants were predominantly transported to the north and northwest of the eruption site. This atmospheric transport pattern likely mitigated the frequency of SO_2 pollution episodes in the densely populated capital area, situated to the northeast of the eruption site. Supplementary Figure S3 illustrates the total probability of above-threshold SO_2 concentrations at ground level during the eruption, as simulated by the IMO dispersion model (Pfeffer et al., 2024). As outlined in Section 3.4, these simulations are used here solely to provide a qualitative indication of the broad plume direction at ground level. The modelled dispersion patterns are consistent with observational data, indicating that the plume most frequently grounded to the north and northwest of the eruption site, and more rarely in the capital area (Fig. S3).

Based on the available evidence, it is likely that the 2021 eruption may have resulted in adverse health impacts among exposed populations. Epidemiological studies by Carlsen et al. (2021a, b) on the 2014–2015 Holuhraun eruption demonstrated a measurable increase in healthcare utilisation for respiratory conditions in the Reykjavík capital area, associated with the presence of the volcanic plume. Exposure to above-threshold SO_2 concentrations was linked to approximately 20% increase in asthma medication dispensations and primary care visits. Furthermore, even modest increases in SO_2 levels were associated with small but statistically significant rises in healthcare usage—approximately a 1% increase per 10 µg/m³ SO_2—suggesting the absence of a safe lower threshold. During the Fagradalsfjall eruption, SO_2 concentrations in populated areas reached levels broadly comparable to those observed during the larger but more distal Holuhraun eruption. Consequently, similar health impacts may be expected, as inferred from the findings of Carlsen et al. (2021a, b). Holuhraun emissions led to 33 exceedances of the SO_2 air quality threshold in Reykjavík, with hourly-mean concentrations peaking at 1400 µg/m³ (Ilyinskaya et al., 2017). In comparison, the Fagradalsfjall eruption caused 31 exceedances, with a maximum of 2400 µg/m³ SO_2 recorded in the community of Vogar (station G2-F). Additionally, Fagradalsfjall caused SO_2 threshold exceedances across all monitored areas within approximately 50 km of the eruption site (areas G1–G5). By definition, there is no safe lower limit for the number of air quality exceedance events. Therefore, all areas that recorded above-threshold pollutant concentrations may have

experienced adverse health effects. Furthermore, although the monitored regions in North and East Iceland (areas G6 and G7) did not register threshold exceedances, potential health impacts in these areas cannot be ruled out. As reported by Carlsen et al. (2021b), even relatively small, above-background increases in SO_2 concentrations during the Holuhraun eruption were associated with measurable health effects.

Given the limited number and scope of health impact studies on previous volcanic eruptions, the potential health implications discussed here should be further investigated through dedicated epidemiological and/or clinical studies focused specifically on the Fagradalsfjall event. Moreover, existing health studies from volcanic regions have primarily concentrated on short-term exposure (hourly and daily), with a gap in research of potential long-term effects. Since the 2021 eruption, ten additional eruptions of similar style and in the same geographic area have occurred. Although each event has been relatively short-lived—ranging from several days to several months—their cumulative impact on air quality and public health may be chronic rather than acute, and thus warrants comprehensive investigation.

Carlsen et al. (2021a) found that when volcanic air pollution events from the Holuhraun eruption were successfully forecast and public advisories were issued, the associated negative health impacts were reduced compared to events that were not forecast. In Iceland, residential buildings are predominantly well-insulated concrete structures with double-glazed windows, offering substantial protection from outdoor air pollution. However, under normal conditions, windows are kept open for ventilation, facilitated by the availability of inexpensive geothermal heating. Additionally, it is common practice for infants to nap outdoors in prams, and for school-aged children to spend breaks outside. Public advisories included simple, easily implemented measures such as keeping windows closed and minimizing outdoor exposure for vulnerable individuals. Given that such basic societal actions have been shown to be effective, it is likely that further improvements in pollution detection—particularly enhancements in spatial resolution—and more effective communication strategies could provide additional protection to the population.

3.5.2 Exposure of eruption site visitors

An interesting aspect of the eruption was that it was generally considered a very positive event by the Icelandic public (Ilyinskaya et al., 2024), and even though it took place in an uninhabited location the site became akin to a densely populated area due to the extremely high number of visitors. The mountainous area had no infrastructure before the eruption and was only accessible by rough mountain tracks. It was unsuitable for an installation of a regulatory air quality network but there were serious concerns about the hazard posed to the visitors by potentially very high SO_2 concentrations. In response, national and local authorities undertook significant efforts to mitigate hazards associated with both volcanic activity and general outdoor hazards. A network of three footpaths was established, originating from designated parking areas (Figure 11a). These footpaths were modified multiple times throughout the eruption as the lava field expanded and optimal viewing locations shifted (Barsotti et al., 2023). In this study, we evaluate the deployment of eruption-response LCS as a means to minimize exposure to hazardous SO_2 levels.

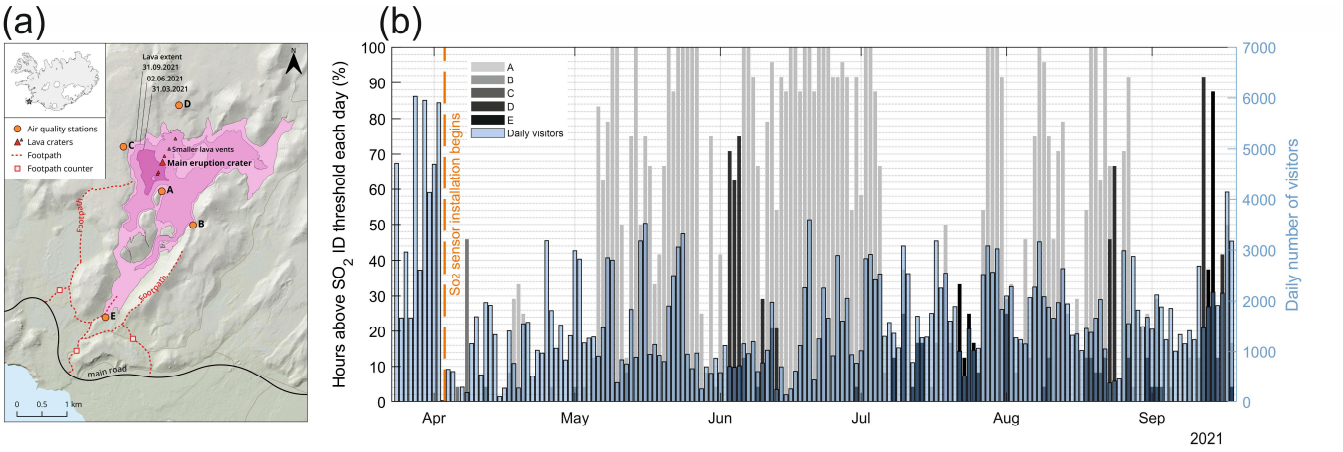

Figure 11: Visitor numbers and potential SO_2 exposure at the Fagradalsfjall eruption site (24 March – 18 September 2024), estimated from LCS that were installed in April (stations A, B) and June (stations C, D, E). Panel (a): Topographic map of the Fagradalsfjall eruption site area showing the locations of the eruption craters, and the evolving extent of the lava field. It also shows the locations of the five LCS stations (A-E), the primary footpaths used by visitors, and the locations of footpath visitor counters. Panel (b): Daily visitor counts and the number of hours per day during which SO_2 concentrations exceeded the ID air quality threshold (350 µg/m³ hourly-mean) at each station. SO_2 exceedance duration is expressed as a percentage of the day (number of hours/24 × 100). Source and copyright of basemap and cartographic elements: Icelandic Met Office & Icelandic Institute of Natural History.

The visitor numbers presented here represent a minimum estimate. Automated footpath counters were installed by the Icelandic Tourist Board on 24 March 2021, with one device placed on each of the main footpaths leading to the eruption site and designated viewpoints (Fig. 11a). These counters (PYRO-Box, Eco Counter, 2021) have a reported accuracy of 95% and a sensing range of 4 meters. While the majority of visitors used the established footpath network, some individuals may have walked outside the detection range of the counters and were therefore not recorded. Additionally, visitors arriving via helicopter sightseeing tours, children being carried, and individuals with authorized vehicle access (e.g., scientists and rescue personnel) were not included in the count. The visitor data also lacked demographic information, preventing any assessment of exposure among more vulnerable age groups. During the monitoring period (24 March to 18 September 2021), the eruption site was visited by approximately 300,000 people, averaging 1,600 visitors per day (Fig. 11b). The highest visitor numbers occurred in the early weeks of the eruption, coinciding with the Easter holiday period, with a daily average of 3,300 visitors and a peak of 6,000 on 28 March.

The five eruption-response LCS were strategically deployed along the main footpaths (Fig. 11a) to ensure proximity to visitors. Figure 11b shows the frequency of ID threshold exceedance events (350 µg/m^3 hourly-mean SO_2) recorded at each of the stations. Station G1-A registered the highest cumulative exposure, with a total of 1,600 hours above the threshold. Stations G1-B, G1-C, and G1-D recorded between 110 and 10 hours of exceedance, while G1-E did not register any exceedances. Stations G1-C and G1-D were more frequently located downwind of the active vents, as supported by the wind rose diagram in Figure B11. Additionally, based on visual observations during this eruption and similar fissure eruptions, a volcanic plume can occasionally collapse and spread laterally. This leads to extremely high concentrations of SO_2 even at locations in close vicinity of but upwind of the volcanic vent.

Visitors were clearly advised to remain upwind of the active craters and lava field. The site was staffed by members of the rescue services and/or rangers, who carried handheld SO_2 LCS to supplement the semi-permanent sensor network. When SO_2 concentrations exceeded threshold levels, visitors were urged to relocate to areas with cleaner air. Although no formal health impact studies have been published to date, anecdotal reports in the Icelandic media suggest that only a small number of individuals sought medical attention after visiting the eruption site, citing symptoms related to gas exposure. This likely represents a very small proportion of the total visitor population. Instances of exposure to unhealthy SO_2 levels may have occurred for several reasons: not all visitors were in proximity to a sensor during their visit, and rapid shifts in wind direction or changes in eruption dynamics occasionally transported SO_2 into areas that had previously been unaffected.

To obtain high-quality datasets with LCS, regular and frequent field calibration against regulatory instruments is essential. However, such calibration is typically feasible only during short-term campaigns at reasonably accessible locations. In this crisis-response scenario, the challenging terrain and limited accessibility of the eruption site precluded field calibration. The primary concerns associated with uncalibrated LCS in emergency contexts are false negatives—where the sensor underreports concentrations that exceed health thresholds—and false positives—where the sensor overreports concentrations that are actually below threshold. False negatives pose a problem by failing to alert individuals to hazardous conditions, while repeated false positives may undermine public trust and reduce compliance with safety advisories.

Both issues can be mitigated by increasing the density of LCS coverage in each monitored area, as was done in this case by supplementing the semi-permanent network with handheld sensors. The likelihood of false positives is further reduced when the alert threshold is set relatively high, as is appropriate when the primary concern is short-term exposure to high concentrations. False negatives are less likely to result in non-compliance at sites used for short visits rather than permanent residence, as visitors are likely to be more willing and able to move.

In conclusion, we suggest that the deployment of the LCS network contributed meaningfully to reducing the SO_2 hazard at the eruption site, given the high frequency of above-threshold SO_2 concentrations and the high number of people within a small area. Such networks are recommended in comparable crisis-response scenarios, provided that careful consideration is given to how the data and resulting alerts are interpreted and communicated. However, their applicability may be less suitable in contexts where chronic exposure among permanent residents is the primary concern.

4 Conclusions

The 2021 eruption of Fagradalsfjall marked the onset of a prolonged eruptive phase on the Reykjanes peninsula, with ten subsequent eruptions occurring through to the time of writing, and continued volcanic unrest. Our findings demonstrate that even a relatively small volcanic event, such as the 2021 eruption, can lead to significant air pollution of SO_2 and PM. Due to its proximity to densely populated areas, the Fagradalsfjall eruption caused elevated pollutant concentrations, and air quality threshold exceedances comparable to those observed during the much larger Holuhraun eruption of 2014–2015. These results suggest that the Fagradalsfjall eruption may have contributed to measurable adverse health effects, warranting further public

health investigations. Moreover, the high frequency of eruptions in this region since 2021 raises the possibility of chronic, low-level air pollution, which should also be examined, particularly given that the ongoing 'Reykjanes Fires' eruptions may continue for several generations.

We showed that even Iceland's exceptionally dense, reference-grade air quality monitoring network was insufficient to fully capture the fine-scale spatial variability of volcanic air pollution episodes. We recommend augmenting existing networks with well-calibrated low-cost sensors (LCS) to enhance spatial coverage, particularly in sensitive locations such as schools and hospitals, where vulnerable populations may be at greater risk. Previous studies on the Holuhraun eruption have demonstrated that public advisories on volcanic air pollution can serve as effective health protection measures. Therefore, improving the spatial resolution of air quality monitoring may further enhance public health outcomes by enabling more targeted and timely advice.

Understanding the volcanic air pollution in a uniquely Icelandic event like the Reykjanes Fires has important implications for how we manage and prepare for other eruptions globally. The fine-scale temporal and spatial variability in pollution dispersion identified in this study highlights the need for further investigation—not only in future Icelandic eruptions but also in other regions exposed to volcanic activity. Enhanced understanding of these dynamics can inform more effective monitoring strategies and public health responses worldwide.

Table S1

Excel file 'Table_S1.xlsx. Information about instrumentation, data completeness, data exclusion, etc, for each SO_2 and PM monitoring station. Summary statistics for SO_2 (hourly-means), PM10, PM2.5 and PM1 (daily-means) data during the background and eruption periods. SO_2 concentration data ($\mu g/m^3$) reported to 2 s.f. Full raw dataset openly available for download from Environment Agency of Iceland https://loftgaedi.is/en.

Figure S1

Animated simulation of the volcanic SO_2 concentration at ground level for the period 28 – 30 May 2021. The colour scale represents the simulated concentrations at ground level (in $\mu g/m^3$) but should be treated as only as a qualitative indication of plume presence at ground-level. The simulation was made by the CALPUFF dispersion model that was used operationally during the 2021 Fagradalsfjall eruption by the Icelandic Met Office. A detailed methodology of the dispersion simulations is in Pfeffer et al., (2024). The data presented in Figure S1 are unpublished data by the Icelandic Meteorological Office.

Figure S2

Animated simulation of the volcanic SO_2 concentration at ground level for the period 18 – 20 July 2021. The colour scale represents the simulated concentrations at ground level (in $\mu g/m^3$) but should be treated as only as a qualitative indication of plume presence at ground-level. The simulation was made by the CALPUFF dispersion model that was used operationally during the 2021 Fagradalsfjall eruption by the Icelandic Met Office. A detailed methodology of the dispersion simulations is in (Pfeffer et al., 2024). The data presented in Figure S2 are unpublished data by the Icelandic Meteorological Office.

Figure S3

Map of the total probability (%) of ground-level SO_2 concentrations exceeding the 350 $\mu g/m^3$ air quality threshold during the 2021 Fagradalsfjall eruption. The map is based on dispersion simulations by the CALPUFF model that was used operationally by the Icelandic Meteorological Office. A detailed methodology of the dispersion simulations is in Pfeffer et al., (2024). The model results are used here for qualitative information about the plume direction (as a yes/no indication of the potential plume presence at ground level) because the model had a reasonable skill in predicting the broad plume direction but a relatively low accuracy in simulating the concentrations of SO_2 at ground level (Pfeffer et al., 2024). The data presented in Figure S3 are unpublished data by the Icelandic Meteorological Office.

Appendix A.

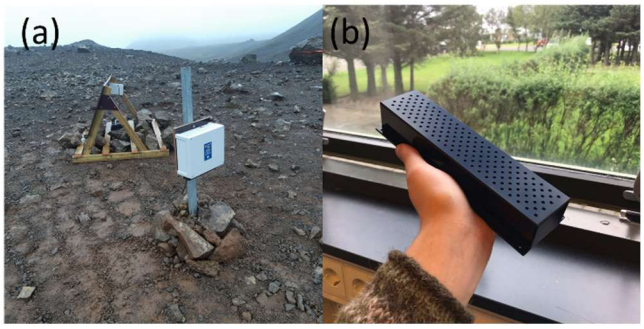

Figure A1 Lower-cost sensors used for the Fagradalsfjall 2021 eruption. Panel (a) shows the instrument installed in the field. The station was powered by a solar panel (triangular trellis at the back of the photo). The air intake was underneath the instrument (the white box at the front of the image). Panel (b) shows the air intake of the sensor. The air intake was designed in-house at the IMO taking into account local conditions, in particular the weather and dust resuspension. The cover was custom-made from Plexiglass with the sensors are recessed behind it to be protected from dust, precipitation, and other potentially damaging environmental factors.

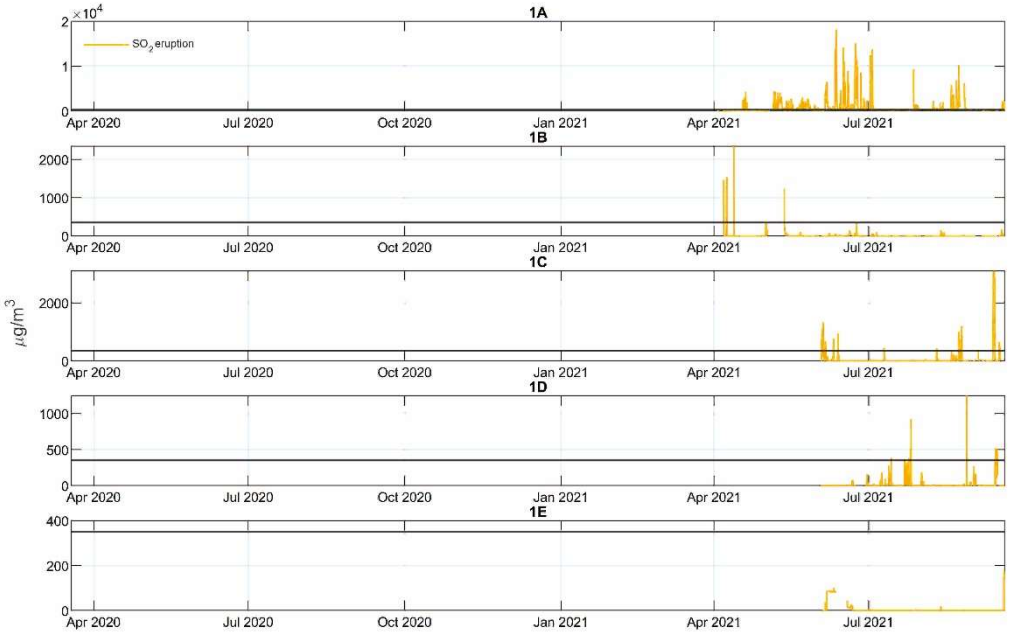

780 **Figure A2 Time series of hourly-mean concentrations SO_2 (µg/m^3), measured by the eruption site stations (G1 A-E) during the 2021 eruption. The stations were not in operation before the eruption an therefore there are no data on pre-eruptive background. The ID air quality threshold of 350 µg/m^3 hourly-mean is shown on all panels with a black horizontal line. Note that the eruption-site LCS have low accuracy and were only used in this study to indicate time periods that were over the ID threshold, the absolute concentration values were not included in the analysis.**

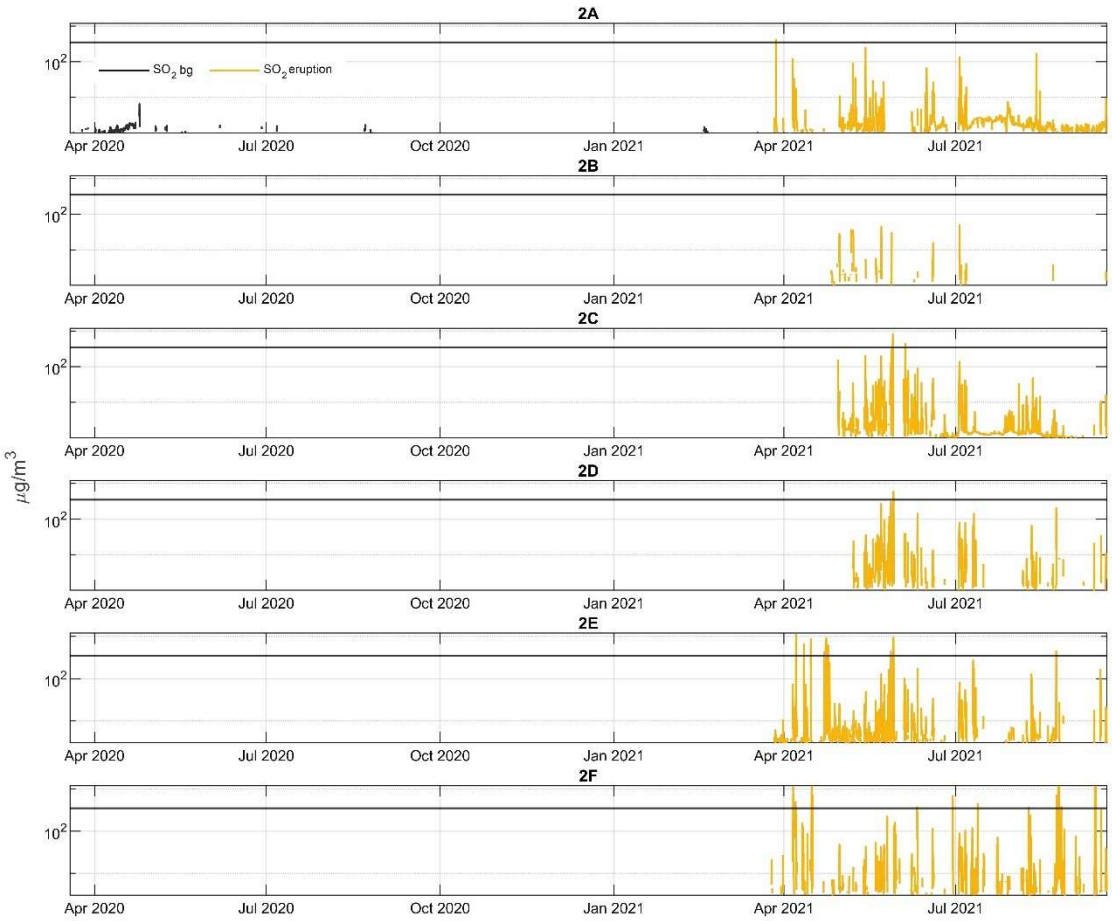

785

Figure A3 Time series of hourly-mean concentrations SO_2 (µg/m^3), measured by Reykjanes peninsula regulatory air quality stations (G2 A-F) during the 2021 eruption and the non-eruptive background in 2020 (bg). The ID air quality threshold of 350 µg/m^3 hourly-mean is shown on all panels with a black horizontal line. Please note the logarithmic y-axis scale.

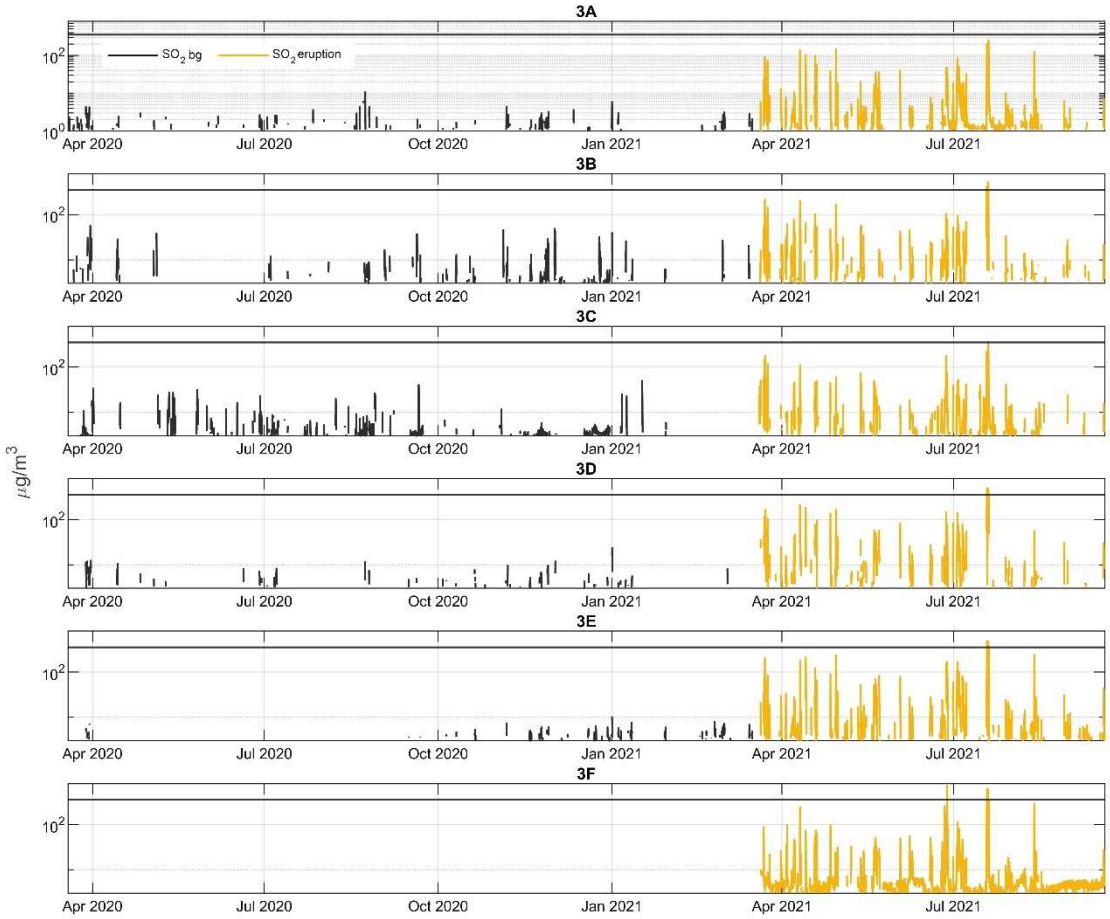

790

Figure A4 Time series of hourly-mean concentrations SO_2 (µg/m^3), measured by Reykjavík capital area regulatory air quality stations (G3 A-F) during the 2021 eruption and the non-eruptive background in 2020 (bg). The ID air quality threshold of 350 µg/m^3 hourly-mean is shown on all panels with a black horizontal line. Please note the logarithmic y-axis scale.

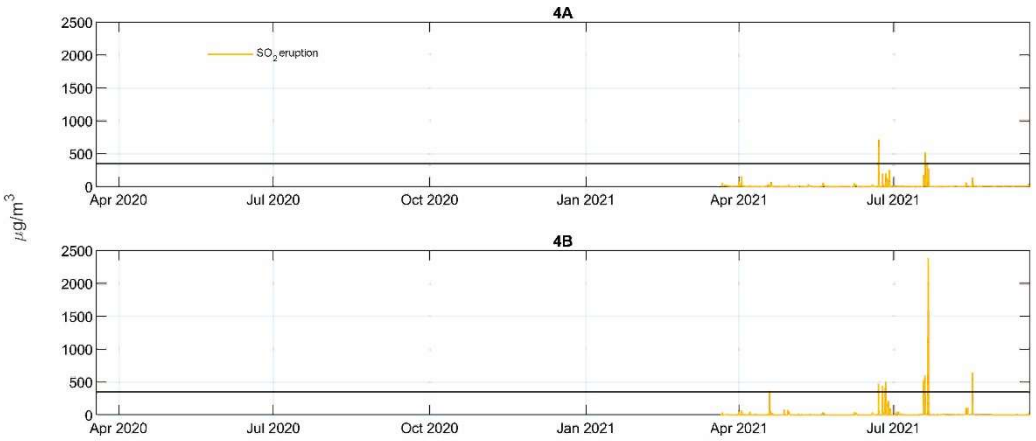

795

Figure A5 Time series of hourly-mean concentrations SO_2 (µg/m^3), measured in Southwest Iceland by regulatory air quality stations (G4 A-B) during the 2021 eruption. The stations were not in operation before the eruption an therefore there are no data on pre-eruptive background. The ID air quality threshold of 350 µg/m^3 hourly-mean is shown on all panels with a black horizontal line.

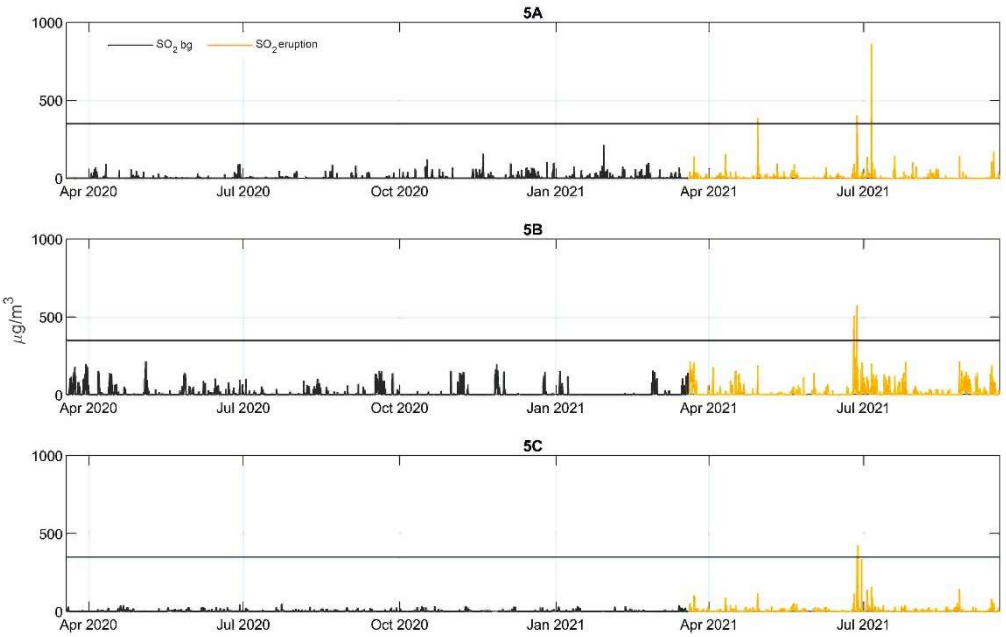

800

Figure A6 Time series of hourly-mean concentrations SO_2 (µg/m^3), measured in Hvalfjörður area by regulatory air quality stations (G5 A-C) during the 2021 eruption and the non-eruptive background in 2020 (bg). The ID air quality threshold of 350 µg/m^3 hourly-mean is shown on all panels with a black horizontal line.

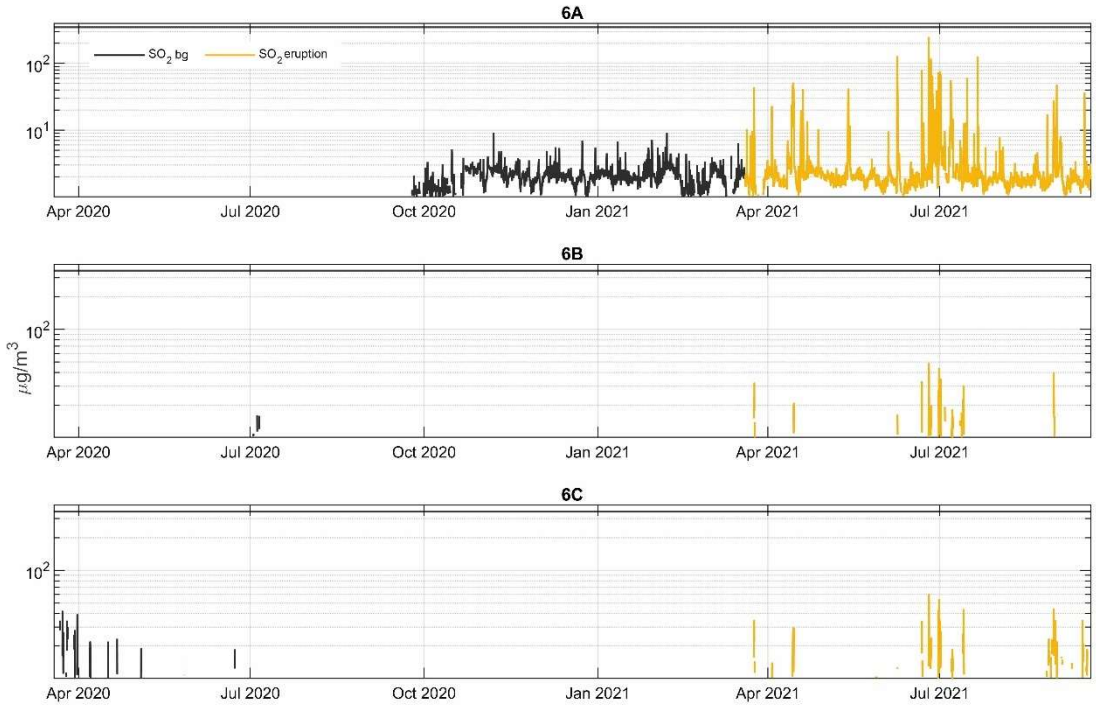

805

Figure A7 Time series of hourly-mean concentrations SO_2 (µg/m^3), measured in North Iceland by regulatory air quality stations (G6 A-C) during the 2021 eruption and the non-eruptive background in 2020 (bg). The ID air quality threshold of 350 µg/m^3 hourly-mean is shown on all panels with a black horizontal line. Please note the logarithmic y-axis scale.

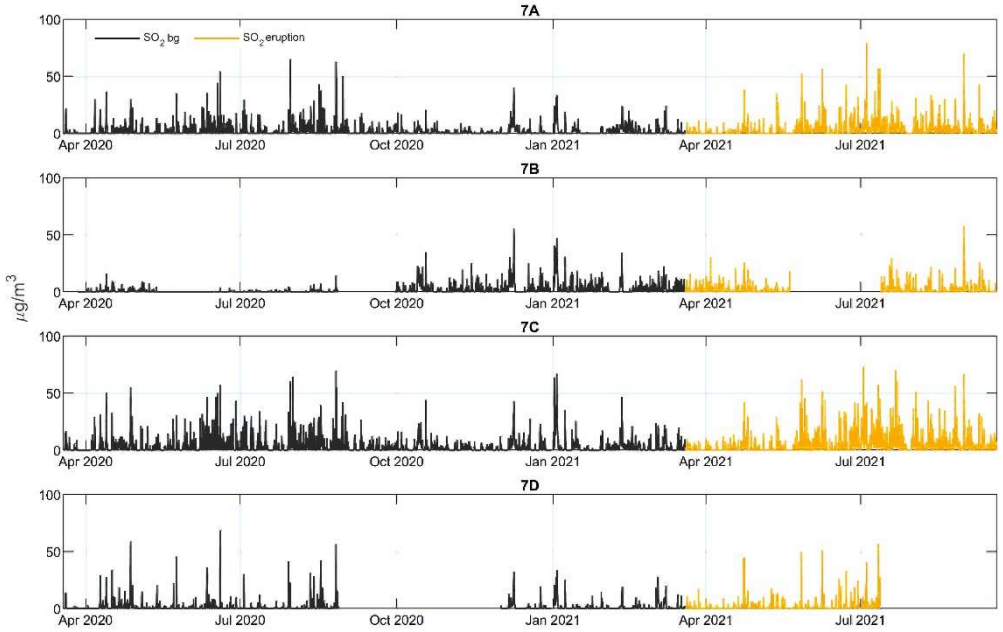

810

Figure A8 Time series of hourly-mean concentrations SO_2 (µg/m^3), measured in East Iceland by regulatory air quality stations (G7 A-D) during the 2021 eruption and the non-eruptive background in 2020 (bg). The ID air quality threshold of 350 µg/m^3 hourly-mean is shown on all panels with a black horizontal line.

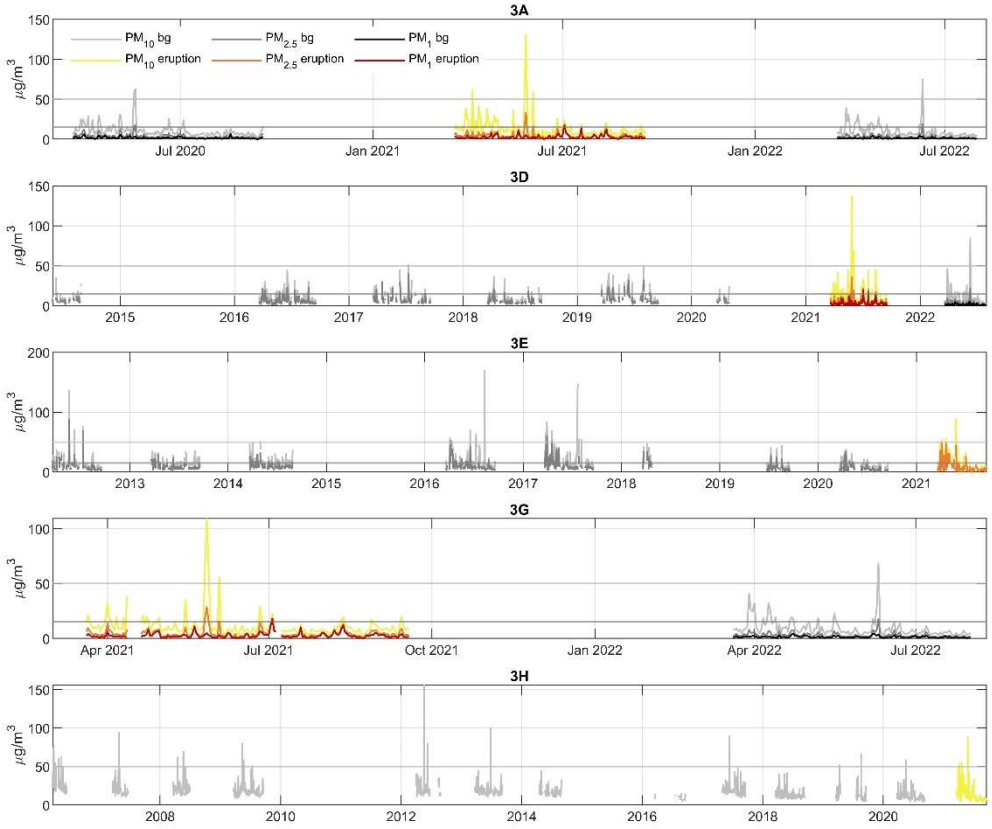

Figure A9 Time series of daily-mean concentrations of PM_{10}, $PM_{2.5}$ and PM_1 (µg/m^3) measured in Reykjavík capital area by regulatory air quality stations (G3 A, D, E, G, H) during the 2021 eruption and in the non-eruptive background (bg). The amount of non-eruptive background data varies between stations based on their installation date. The figures only include data for the period 19 March 20:00 – 19 September 00:00 UTC in each year, i.e. the period corresponding to the calendar dates and months of the 2021 eruption. See main text for the justification of this approach. The figures show the ID air quality thresholds for PM_{10} and $PM_{2.5}$ of 50 and 15 µg/m^3 daily-mean, respectively as grey horizontal lines. For PM_1, air quality thresholds have not been determined.

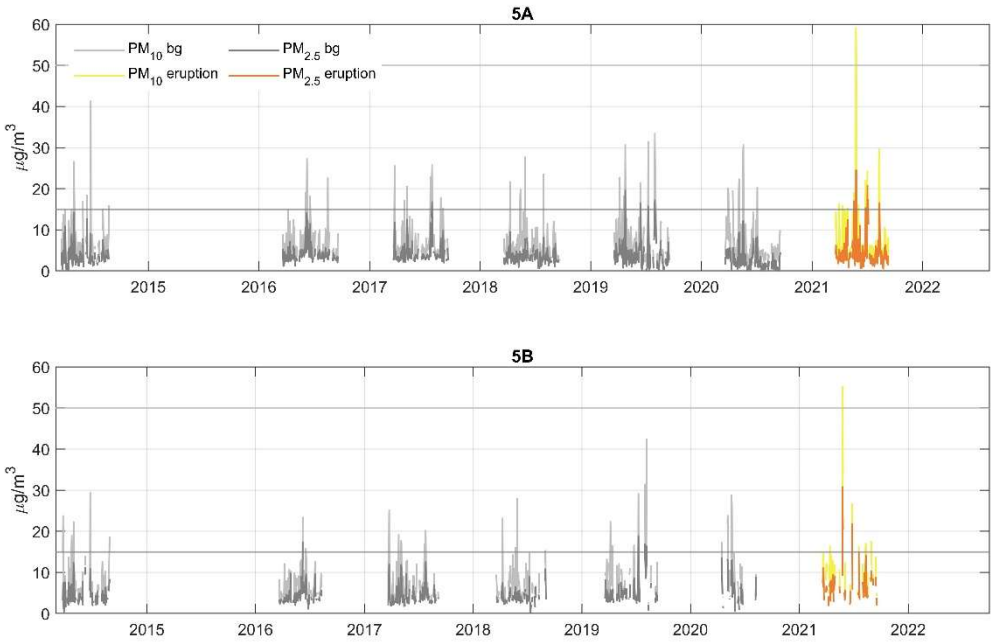

Figure A10 Time series of daily-mean concentrations of PM_{10}, and $PM_{2.5}$ (µg/m^3) measured in Hvalfjörður area by regulatory air quality stations (G5 A, B) during the 2021 eruption and in the non-eruptive background (bg). PM_1 was not measured at these stations. The amount of non-eruptive background data varies between stations based on their installation date. The figures only include data for the period 19 March 20:00 – 19 September 00:00 UTC in each year, i.e. the period corresponding to the calendar dates and months of the 2021 eruption. See main text for the justification of this approach. The figures show the ID air quality thresholds for PM_{10} and $PM_{2.5}$ of 50 and 15 µg/m^3 daily-mean, respectively as grey horizontal lines.

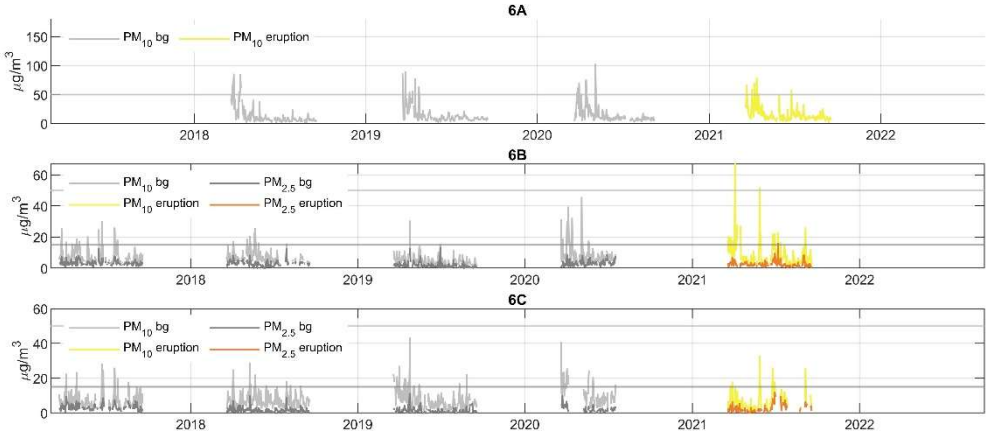

Figure A11 Time series of daily-mean concentrations of PM_{10}, and $PM_{2.5}$ (µg/m^3) measured in North Iceland by regulatory air quality stations (G6 A, B, C) during the 2021 eruption and in the non-eruptive background (bg). PM_1 was not measured at these stations. The figures only include data for the period 19 March 20:00 – 19 September 00:00 UTC in each year, i.e. the period corresponding to the calendar dates and months of the 2021 eruption. See main text for the justification of this approach. The figures show the ID air quality thresholds for PM_{10} and $PM_{2.5}$ of 50 and 15 µg/m^3 daily-mean, respectively as grey horizontal lines.

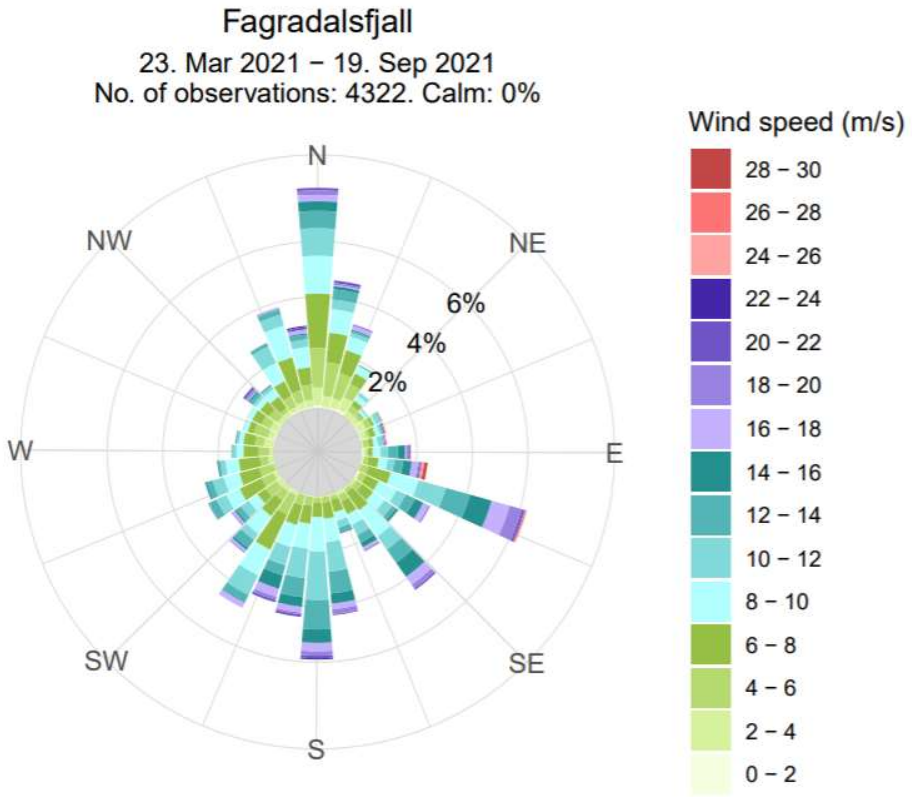

Figure A12 Wind rose shows wind direction (wind coming from) and wind speed measured by Icelandic Meteorological Office weather station at the Fagradalsfjall eruption site 23 March – 19 September 2021.

Data availability

Full dataset of measured SO_2, PM_{10}, $PM_{2.5}$ and PM_1 concentrations is openly available for download from the Environment Agency of Iceland https://loftgaedi.is/en.

Author contributions

RCWW performed the original data analysis and drafted the original manuscript and figures. SB, MAP, TR and AS contributed to data interpretation and manuscript drafting. EI finalised the data analysis, the manuscript and produced Figs. 2-7, 9 and Appendix A1-A11. RHTh produced Figs. 1, 8, and 9. TH, GMG and MAP designed, built and maintained IMO's measurement and data systems. TJ contributed access to and information on the regulatory AQ network and quality-controlled data. DF and RHTh led on the ArcGIS ArcMap analysis methodology. GGS supplied the data from footpath counters. All coauthors contributed to draft review and editing.

Competing interests

The authors declare that they have no conflict of interest.

Acknowledgements

The authors would like to thank Kristín Björg Ólafsdóttir from the Icelandic Meteorological Office for analysis of wind data and creation of the wind rose in Appendix A Fig. A12. Bogi Brynjar Björnsson at the Icelandic Meteorological Office is thanked for the preparation of Supplementary Figure S3. Microsoft Copilot (GPT-4) was used for English language editing, proofreading, and improving sentence clarity and structure; all content edited by Microsoft Copilot (GPT-4) was critically reviewed and approved by the authors.

Financial support

RCWW was funded by the Leeds-York Natural Environment Research Council (NERC) Doctoral Training Partnership (DTP) NE/L002574/1, in CASE partnership with the Icelandic Meteorological Office. TJR was funded by the ANR Projet de Recherche Collaborative VOLC-HAL-CLIM (Volcanic Halogens: from Deep Earth to Atmospheric Impacts) ANR-18-CE01-0018, and Labex Orléans Labex VOLTAIRE (VOLatils-Terre Atmosphère Interactions–Ressources et Environnement, ANR-10-LABX-100-0). EI acknowledges NERC Centre for Observation and Modelling of Earthquakes, Volcanoes and Tectonics (COMET+), a partnership between UK Universities and the British Geological Survey; NERC Highlight Topic V-PLUS NE/S00436X/1 and NERC Urgency Grant NE/Z000262/1 “Chemistry of emissions at lava-urban interfaces”.

References

Apte, J. S. and Manchanda, C.: High-resolution urban air pollution mapping, Science, 385, 380–385, https://doi.org/10.1126/science.adq3678, 2024.

Barsotti, S.: Probabilistic hazard maps for operational use: the case of SO2 air pollution during the Holuhraun eruption (Bárðarbunga, Iceland) in 2014–2015, Bull. Volcanol., 82, 56, https://doi.org/10.1007/s00445-020-01395-3, 2020.

Barsotti, S., Parks, M. M., Pfeffer, M. A., Óladóttir, B. A., Barnie, T., Titos, M. M., Jónsdóttir, K., Pedersen, G. B. M., Hjartardóttir, Á. R., Stefansdóttir, G., Johannsson, T., Arason, Þ., Gudmundsson, M. T., Oddsson, B., Þrastarson, R. H., Ófeigsson, B. G., Vogfjörd, K., Geirsson, H., Hjörvar, T., von Löwis, S., Petersen, G. N., and Sigurðsson, E. M.: The eruption in Fagradalsfjall (2021, Iceland): how the operational monitoring and the volcanic hazard assessment contributed to its safe access, Nat. Hazards, https://doi.org/10.1007/s11069-022-05798-7, 2023.

Brauer, M., Roth, G. A., Aravkin, A. Y., Zheng, P., Abate, K. H., Abate, Y. H., Abbafati, C., Abbasgholizadeh, R., Abbasi, M. A., Abbasian, M., Abbasifard, M., Abbasi-Kangevari, M., ElHafeez, S. A., Abd-Elsalam, S., Abdi, P., Abdollahi, M., Abdoun, M., Abdulah, D. M., Abdullahi, A., Abebe, M., Abedi, A., Abedi, A., Abegaz, T. M., Zuñiga, R. A. A., Abiodun, O., Abiso, T. L., Aboagye, R. G., Abolhassani, H., Abouzid, M., Aboye, G. B., Abreu, L. G., Abualruz, H., Abubakar, B., Abu-Gharbieh, E., Abukhadijah, H. J. J., Aburuz, S., Abu-Zaid, A., Adane, M. M., Addo, I. Y., Addolorato, G., Adedoyin, R. A., Adekanmbi, V., Aden, B., Adetunji, J. B., Adeyeoluwa, T. E., Adha, R., Adibi, A., Adnani, Q. E. S., Adzigbli, L. A., Afolabi, A. A., Afolabi, R. F., Afshin, A., Afyouni, S., Afzal, M. S., Afzal, S., Agampodi, S. B., Agbozo, F., Aghamiri, S., Agodi, A., Agrawal, A., Agyemang-Duah, W., Ahinkorah, B. O., Ahmad, A., Ahmad, D., Ahmad, F., Ahmad, N., Ahmad, S., Ahmad, T., Ahmed, A., Ahmed, A., Ahmed, A., Ahmed, L. A., Ahmed, M. B., Ahmed, S., Ahmed, S. A., Ajami, M., Akalu, G. T., Akara, E. M., Akbarialiabad, H., Akhlaghi, S., Akinosoglou, K., Akinyemiju, T., Akkaif, M. A., Akkala, S., Akombi-Inyang, B., Awaidy, S. A., Hasan, S. M. A., Alahdab, F., AL-Ahdal, T. M. A., Alalalmeh, S. O., Alalwan, T. A., Al-Aly, Z., Alam, K., Alam, N., Alanezi, F. M., Alanzi, T. M., Albakri, A., AlBataineh, M. T., Aldhaleei, W. A., et al.: Global burden and strength of evidence for 88 risk factors in 204 countries and 811 subnational locations, 1990–2021: a systematic analysis for the Global Burden of Disease Study 2021, The Lancet, 403, 2162–2203, https://doi.org/10.1016/S0140-6736(24)00933-4, 2024.

Butwin, M. K., von Löwis, S., Pfeffer, M. A., and Thorsteinsson, T.: The effects of volcanic eruptions on the frequency of particulate matter suspension events in Iceland, J. Aerosol Sci., 128, 99–113, 2019.

Caplin, A., Ghandehari, M., Lim, C., Glimcher, P., and Thurston, G.: Advancing environmental exposure assessment science to benefit society, Nat. Commun., 10, 1236, https://doi.org/10.1038/s41467-019-09155-4, 2019.

Carlsen, H. K. and Thorsteinsson, T.: Associations between PM10 from Traffic, Resuspension, Sand Storms and Volcanic Sources and Asthma Drugs Dispensing, In Review, https://doi.org/10.21203/rs.3.rs-1017409/v1, 2021.

Carlsen, H. K., Ilyinskaya, E., Baxter, P. J., Schmidt, A., Thorsteinsson, T., Pfeffer, M. A., Barsotti, S., Dominici, F., Finnbjornsdottir, R. G., Jóhannsson, T., Aspelund, T., Gislason, T., Valdimarsdóttir, U., Briem, H., and Gudnason, T.: Increased respiratory morbidity associated with exposure to a mature volcanic plume from a large Icelandic fissure eruption, Nat. Commun., 12, 2161, https://doi.org/10.1038/s41467-021-22432-5, 2021a.

Carlsen, H. K., Valdimarsdóttir, U., Briem, H., Dominici, F., Finnbjornsdottir, R. G., Jóhannsson, T., Aspelund, T., Gislason, T., and Gudnason, T.: Severe volcanic \ceSO2 exposure and respiratory morbidity in the Icelandic population–a register study, Environ. Health, 20, 1–12, 2021b.

Crawford, B., Hagan, D. H., Grossman, I., Cole, E., Holland, L., Heald, C. L., and Kroll, J. H.: Mapping pollution exposure and chemistry during an extreme air quality event (the 2018 Kīlauea eruption) using a low-cost sensor network, Proc. Natl. Acad. Sci., 118, 2021.

Crilley, L. R., Shaw, M., Pound, R., Kramer, L. J., Price, R., Young, S., Lewis, A. C., and Pope, F. D.: Evaluation of a low-cost optical particle counter (Alphasense OPC-N2) for ambient air monitoring, Atmospheric Meas. Tech., 709–720, 2018.

Felton, D., Grange, G., Damby, D., Bronstein, A., and Spyker, D.: Sulfur dioxide monitoring associated with the 2018 Kilauea Lower East Rift Zone Eruption, International Union of Toxicology (IUTOX) 15th International Congress of Toxicology, Honolulu, HI, USA, 2019.

Freire, S., Florczyk, A. J., Pesaresi, M., and Sliuzas, R.: An Improved Global Analysis of Population Distribution in Proximity to Active Volcanoes, 1975–2015, ISPRS Int. J. Geo-Inf., 8, 341, https://doi.org/10.3390/ijgi8080341, 2019.

Gan, T., Chu, J., Bambrick, H., Guo, X., and Hu, W.: Long-term exposure to PM1 and liver cancer mortality: Insights into the role of smaller particulate fractions, Ecotoxicol. Environ. Saf., 300, 118467, https://doi.org/10.1016/j.ecoenv.2025.118467, 2025.

Gíslason, S. R., Stefánsdóttir, G., Pfeffer, M. A., Barsotti, S., Jóhannsson, Th., Galeczka, I., Bali, E., Sigmarsson, O., Stefánsson, A., Keller, N. S., Sigurdsson, á., Bergsson, B., Galle, B., Jacobo, V. C., Arellano, S., Aiuppa, A., Jónasdóttir, E. B., Eiríksdóttir, E. S., Jakobsson, S., Guðfinnsson, G. H., Halldórsson, S. A., Gunnarsson, H., Haddadi, B., Jónsdóttir, I., Thordarson, Th., Riishuus, M., Högnadóttir, Th., Dürig, T., Pedersen, G. B. M., Höskuldsson, á., and Gudmundsson, M. T.: Environmental pressure from the 2014–15 eruption of Bárðarbunga volcano, Iceland, Geochem. Perspect. Lett., 84–93, https://doi.org/10.7185/geochemlet.1509, 2015.

Green, J. R., Fiddler, M. N., Holloway, J. S., Fibiger, D. L., McDuffie, E. E., Campuzano-Jost, P., Schroder, J. C., Jimenez, J. L., Weinheimer, A. J., Aquino, J., and others: Rates of wintertime atmospheric \ceSO2 oxidation based on aircraft observations during clear-sky conditions over the eastern United States, J. Geophys. Res. Atmospheres, 124, 6630–6649, 2019.

Guo, H., Li, X., Wei, J., Li, W., Wu, J., and Zhang, Y.: Smaller particular matter, larger risk of female lung cancer incidence? Evidence from 436 Chinese counties, BMC Public Health, 22, 344, https://doi.org/10.1186/s12889-022-12622-1, 2022.

Horwell, C. J., Elias, T., Covey, J., Bhandari, R., and Truby, J.: Perceptions of volcanic air pollution and exposure reduction practices on the Island of Hawai‘i: Working towards socially relevant risk communication, Int. J. Disaster Risk Reduct., 95, 103853, https://doi.org/10.1016/j.ijdrr.2023.103853, 2023.

Icelandic Directive: Reglugerð um brennisteinsdíoxíð, köfnunarefnisdíoxíð og köfnunarefnisoxíð, bensen, kolsýring, svifryk og blý í andrúmsloftinu, B-Deild, Nr.920, 2016.

Ilyinskaya, E., Martin, R. S., and Oppenheimer, C.: Aerosol formation in basaltic lava fountaining: Eyjafjallajökull volcano, Iceland, J Geophys Res, 117, D00U27, https://doi.org/10.1029/2011JD016811, 2012.

Ilyinskaya, E., Schmidt, A., Mather, T. A., Pope, F. D., Witham, C., Baxter, P., Jóhannsson, T., Pfeffer, M., Barsotti, S., Singh, A., Sanderson, P., Bergsson, B., McCormick Kilbride, B., Donovan, A., Peters, N., Oppenheimer, C., and Edmonds, M.: Understanding the environmental impacts of large fissure eruptions: Aerosol and gas emissions from the 2014–2015 Holuhraun eruption (Iceland), Earth Planet. Sci. Lett., 472, 309–322, https://doi.org/10.1016/j.epsl.2017.05.025, 2017.

Ilyinskaya, E., Mason, E., Wieser, P. E., Holland, L., Liu, E. J., Mather, T. A., Edmonds, M., Whitty, R. C. W., Elias, T., Nadeau, P. A., Schneider, D., McQuaid, J. B., Allen, S. E., Harvey, J., Oppenheimer, C., Kern, C., and Damby, D.: Rapid metal pollutant deposition from the volcanic plume of Kīlauea, Hawai’i, Commun. Earth Environ., 2, 1–15, https://doi.org/10.1038/s43247-021-00146-2, 2021.

Ilyinskaya, E., Snæbjarnarson, V., Carlsen, H. K., and Oddsson, B.: Brief communication: Small-scale geohazards cause significant and highly variable impacts on emotions, Nat. Hazards Earth Syst. Sci., 24, 3115–3128, https://doi.org/10.5194/nhess-24-3115-2024, 2024.

Longo, B. M.: The Kilauea Volcano Adult Health Study, Nurs. Res., 58, 2009.

Longo, B. M., Rossignol, A., and Green, J. B.: Cardiorespiratory health effects associated with sulphurous volcanic air pollution, Public Health, 122, 809–820, https://doi.org/doi: DOI: 10.1016/j.puhe.2007.09.017, 2008.

Martin, R. S., Ilyinskaya, E., Sawyer, G. M., Tsanev, V. I., and Oppenheimer, C.: A re-assessment of aerosol size distributions from Masaya volcano (Nicaragua), Atmos. Environ., 45, 547–560, https://doi.org/doi: DOI: 10.1016/j.atmosenv.2010.10.049, 2011.

Mason, E., Wieser, P. E., Liu, E. J., Edmonds, M., Ilyinskaya, E., Whitty, R. C. W., Mather, T. A., Elias, T., Nadeau, P. A., Wilkes, T. C., McGonigle, A. J. S., Pering, T. D., Mims, F. M., Kern, C., Schneider, D. J., and Oppenheimer, C.: Volatile metal emissions from volcanic degassing and lava–seawater interactions at Kīlauea Volcano, Hawai'i, Commun. Earth Environ., 2, 1–16, https://doi.org/10.1038/s43247-021-00145-3, 2021.

Mather, T. A., Pyle, D. M., and Oppenheimer, C.: Tropospheric volcanic aerosol, in: Geophysical Monograph Series, vol. 139, edited by: Robock, A. and Oppenheimer, C., American Geophysical Union, Washington, D. C., 189–212, https://doi.org/10.1029/139GM12, 2003.

Pattantyus, A. K., Businger, S., and Howell, S. G.: Review of sulfur dioxide to sulfate aerosol chemistry at Kīlauea Volcano, Hawai'i, Atmos. Environ., 185, 262–271, https://doi.org/10.1016/j.atmosenv.2018.04.055, 2018.

Pfeffer, M. A., Arellano, S., Barsotti, S., Petersen, G. N., Barnie, T., Ilyinskaya, E., Hjörvar, T., Bali, E., Pedersen, G. B. M., Guðmundsson, G. B., Vogfjorð, K., Ranta, E. J., Óladóttir, B. A., Edwards, B. A., Moussallam, Y., Stefánsson, A., Scott, S. W., Smekens, J.-F., Varnam, M., and Titos, M.: SO2 emission rates and incorporation into the air pollution dispersion forecast during the 2021 eruption of Fagradalsfjall, Iceland, J. Volcanol. Geotherm. Res., 449, 108064, https://doi.org/10.1016/j.jvolgeores.2024.108064, 2024.

Schmidt, A., Leadbetter, S., Theys, N., Carboni, E., Witham, C. S., Stevenson, J. A., Birch, C. E., Thordarson, T., Turnock, S., Barsotti, S., Delaney, L., Feng, W., Grainger, R. G., Hort, M. C., Höskuldsson, Á., Ialongo, I., Ilyinskaya, E., Jóhannsson, T., Kenny, P., Mather, T. A., Richards, N. A. D., and Shepherd, J.: Satellite detection, long-range transport and air quality impacts of volcanic sulfur dioxide from the 2014–15 flood lava eruption at Bárðarbunga (Iceland), J. Geophys. Res. Atmospheres, 2015JD023638, https://doi.org/10.1002/2015JD023638, 2015.

Sigurgeirsson, M. and Einarsson, S.: Reykjanes and Svartsengi volcanic systems, in: Catalogue of Icelandic Volcanoes, IMO, UI and CPD-NCIP, 2019.

Sokhi, R. S., Moussiopoulos, N., Baklanov, A., Bartzis, J., Coll, I., Finardi, S., Friedrich, R., Geels, C., Grönholm, T., Halenka, T., Ketzel, M., Maragkidou, A., Matthias, V., Moldanova, J., Ntziachristos, L., Schäfer, K., Suppan, P., Tsegas, G., Carmichael, G., Franco, V., Hanna, S., Jalkanen, J.-P., Velders, G. J. M., and Kukkonen, J.: Advances in air quality research – current and emerging challenges, Atmospheric Chem. Phys., 22, 4615–4703, https://doi.org/10.5194/acp-22-4615-2022, 2022.

Statistics Iceland: Average annual population by municipality, age and sex 1998-2022 - Current municipalities, 2022.

Stewart, C., Damby, D. E., Horwell, C. J., Elias, T., Ilyinskaya, E., Tomašek, I., Longo, B. M., Schmidt, A., Carlsen, H. K., Mason, E., Baxter, P. J., Cronin, S., and Witham, C.: Volcanic air pollution and human health: recent advances and future directions, Bull. Volcanol., 84, 11, https://doi.org/10.1007/s00445-021-01513-9, 2021.

Tam, E., Miike, R., Labrenz, S., Sutton, A. J., Elias, T., Davis, J., Chen, Y.-L., Tantisira, K., Dockery, D., and Avol, E.: Volcanic air pollution over the Island of Hawai'i: Emissions, dispersal, and composition. Association with respiratory symptoms and lung function in Hawai'i Island school children, Environ. Int., 92–93, 543–552, https://doi.org/10.1016/j.envint.2016.03.025, 2016.

US EPA National Center for Environmental Assessment, R. T. P. N.: 2008 Final Report: Integrated Science Assessment (ISA) for Sulfur Oxides – Health Criteria, 2008.

Whitty, R., Pfeffer, M., Ilyinskaya, E., Roberts, T., Schmidt, A., Barsotti, S., Strauch, W., Crilley, L., Pope, F., Bellanger, H., Mendoza, E., Mather, T., Liu, E., Peters, N., Taylor, I., Francis, H., Leiva, X. H., Lynch, D., Nobert, S., and Baxter, P.: Effectiveness of low-cost air quality monitors for identifying volcanic SO_2 and PM downwind from Masaya volcano, Nicaragua, Volcanica, 5, 33–59, https://doi.org/10.30909/vol.05.01.3359, 2022.

Whitty, R. C. W., Ilyinskaya, E., Mason, E., Wieser, P. E., Liu, E. J., Schmidt, A., Roberts, T., Pfeffer, M. A., Brooks, B., Mather, T. A., Edmonds, M., Elias, T., Schneider, D. J., Oppenheimer, C., Dybwad, A., Nadeau, P. A., and Kern, C.: Spatial and Temporal Variations in SO2 and PM2.5 Levels Around Kīlauea Volcano, Hawai'i During 2007–2018, Front. Earth Sci., 8, https://doi.org/10.3389/feart.2020.00036, 2020.

World Health Organization: WHO global air quality guidelines: particulate matter (PM2.5 and PM10), ozone, nitrogen dioxide, sulfur dioxide and carbon monoxide, World Health Organization, xxi, 267 pp., 2021.

Yang, M., Chu, C., Bloom, M. S., Li, S., Chen, G., Heinrich, J., Markevych, I., Knibbs, L. D., Bowatte, G., Dharmage, S. C., and others: Is smaller worse? New insights about associations of PM\textsubscript1 and respiratory health in children and adolescents, Environ. Int., 120, 516–524, 2018.

Zhang, Y., Ding, Z., Xiang, Q., Wang, W., Huang, L., and Mao, F.: Short-term effects of ambient PM1 and PM2.5 air pollution on hospital admission for respiratory diseases: Case-crossover evidence from Shenzhen, China, Int. J. Hyg. Environ. Health, 224, 113418, https://doi.org/10.1016/j.ijheh.2019.11.001, 2020.